HUMAN POSTURAL CONTROL CHARACTERISTICS DURING FORWARD STEPPING: RELATIONSHIP BETWEEN COM AND BODY ACCELERATIONS, TRUNK ACCELERATION VARIABILITY AND COP CHARACTERISTICS

by

Jungmok Han

A Thesis submitted to
the Faculty of Graduate Studies
In Partial Fulfillment of the Requirements for the Degree of

MASTER OF SCIENCE

Department of Electrical and Computer Engineering
University of Manitoba
Winnipeg, Manitoba

Jungmok Han © 2007

THE UNIVERSITY OF MANITOBA

FACULTY OF GRADUATE STUDIES

*****

COPYRIGHT PERMISSION

HUMAN POSTURAL CONTROL CHARACTERISTICS DURING FORWARD STEPPING: RELATIONSHIP BETWEEN COM AND BODY ACCELERATIONS, TRUNK ACCELERATION VARIABILITY AND COP CHARACTERISTICS

BY

Jungmok Han

A Thesis/Practicum submitted to the Faculty of Graduate Studies of The University of Manitoba in partial fulfillment of the requirement of the degree

MASTER OF SCIENCE

Jungmok Han © 2007

Permission has been granted to the University of Manitoba Libraries to lend a copy of this thesis/practicum, to Library and Archives Canada (LAC) to lend a copy of this thesis/practicum, and to LAC's agent (UMI/ProQuest) to microfilm, sell copies and to publish an abstract of this thesis/practicum.

This reproduction or copy of this thesis has been made available by authority of the copyright owner solely for the purpose of private study and research, and may only be reproduced and copied as permitted by copyright laws or with express written authorization from the copyright owner.

THE UNIVERSITY OF MANITOBA

FACULTY OF GRADUATE STUDIES

*****

COPYRIGHT PERMISSION

HUMAN POSTURAL CONTROL CHARACTERISTICS DURING FORWARD STEPPING: RELATIONSHIP BETWEEN COM AND BODY ACCELERATIONS, TRUNK ACCELERATION VARIABILITY AND COP CHARACTERISTICS

BY

JUNGMOK HAN

A Thesis/Practicum submitted to the Faculty of Graduate Studies of the University of Manitoba in partial fulfillment of the requirement of the degree

Of

MASTER OF SCIENCE

Jungmok Han © 2007

Permission has been granted to the Library of the University of Manitoba to lend or sell copies of this thesis/practicum, to the National Library of Canada to microfilm this thesis and to lend or sell copies of the film, and to University Microfilm Inc. to publish an abstract of this thesis/practicum.

This reproduction or copy of this thesis has been made available by authority of the copyright owner solely for the purpose of private study and research, and may only be reproduced and copied as permitted by copyright laws or with express written authorization from the copyright owner.

ABSTRACT

Detecting and monitoring the decline of balance and mobility skills is crucial, especially for the elderly, as it may lead to falls causing injury, death, physical dependence and/or hospitalization. This thesis is an attempt to investigate and develop clinically relevant and objective tools to assess balance disorder.

Firstly, a parabolic model was used to estimate the center of body mass (COM) trajectory during forward stepping, using the body segments' accelerations, which were measured by inexpensive and portable accelerometers placed on the trunk and swing leg. Three different models (fuzzy inference model, sum-of-sines model and parabolic model) were employed, using paced and voluntary forward stepping performed on different support surfaces and with different speeds of stepping. The results are encouraging for the use of the proposed model as a mean to estimate the COM trajectory during forward stepping.

Secondly, trunk acceleration variability was studied in order to examine whether the variability may indicate adaptability of human balance control. An increase in trunk acceleration variability and significantly higher trunk acceleration variability in the M-L direction than that in the A-P direction were found in one task only (stepping on a fixed surface at a normal speed). The results showed that the variability may distinguish normal stepping from other stepping tasks and the M-L trunk acceleration may represent a different aspect of motor control from the A-P trunk acceleration.

Finally, the use of linear and nonlinear dynamic tools to extract characteristic features of postural sway was investigated; sway path length and Rényi dimension, respectively.

The center of foot pressure (COP) trajectory measured by Force Sensing Application (FSA) mat during forward stepping was used as input signal. The results suggest that the COP trajectories' Rényi dimension and sway path length provide different indications of postural control system characteristics between different task demands.

ACKNOWLEDGEMENTS

I wish to express my heartfelt gratitude to my two advisors, Dr. Zahra Moussavi and Dr. Tony Szturm, for reading on my numerous revisions and helping me learn. They have inspired me to greater efforts during Master of Science program, and this research would not have been possible without them.

I would like to thank my fellow student in the department, Aimee Betker, for finding grammar errors in my thesis, and presenting useful seminars during regular group meetings on Friday.

I wish to personally thank Dr. Barbara Shay at the Bannatyne campus for her generous consent on the use of VICON motion capture systems and the laboratory.

I would like to thank my fellow students at the Bannatyne campus, Manish Raghunath, Archana Arun and Ankur Desai, for their help on preparing and setting up the experiments.

Special thanks go to all subjects for participating in repeated stepping trials. They were generous enough to spare their time for us.

I would like to thank my wife and her parents for encouraging and understanding my work. Thanks also go to my two sons, Jeremy (Tae Kyung) and Brandon (Tae Kang), for making me smile.

Finally, I wish to show my gratitude to my parents for supporting me to finish my study. I can not thank them enough.

TABLE OF CONTENTS

LIST OF FIGURES

LIST OF TABLES

CHAPTER 1

INTRODUCTION

1.1 MOTIVATION

Detecting and monitoring the decline of balance and mobility skills is crucial, especially for the elderly, as it may lead to falls causing injury, death, physical dependence and/or hospitalization. Good balance is important when performing activities of daily living; this is particularly prevalent when walking outdoors and when confronting stumbles, unexpected disturbances and various supporting surfaces [Rogers *et al.*, 2003]. To maintain balance, our central nervous system depends on spatial and temporal information from internal and external reference frames. Information gathered from the sensors is synthesized in the higher level cognitive system to maintain and recover standing and walking balance [Allum and Honegger, 1998]. Balance impairment and mobility limitations occur as a result of: a) a singular disorder or condition, such as stroke, traumatic brain injury, diabetes or Parkinson's disease, and b) the contribution of several modest neuromuscular deficits, any one of which alone might not have caused falling. Many factors can contribute to the degradation of our balance system, including an aging-related decrease in sensory information and the processing of that information, and frail conditions such as neurological and musculoskeletal disorders.

Falls are a major source of disability and death in the elderly. During the period from 1998 to 2003, fall-related hospitalization cases for the elderly in non-residential care varied from 40,000 to 43,000 per year; in residential care, cases ranged from 6,000 to

9,000 per year [Scott *et al.*, 2005]. In Canada alone, more than 7,000 Canadians aged 65 and over died as a direct result of a fall during the period from 1997 to 2002 [Scott *et al.*, 2005]. Early diagnosis and detection of balance impairments are important for management and prevention of further degradation and fall injuries. A practical analysis system is required to assess the level of sensory information for diagnosis and detection of sensory deficiencies. For a clinician to perform a routine assessment, the equipment used must be portable, inexpensive and easy to use; however, this is generally not the case. Although normal, firm and fixed surfaces are a task condition that is commonly employed, unpredictable surfaces, such as a foam pad (sponge), need to be considered to emulate an outdoor terrain environment. It is important to consider velocity conditions in stepping or walking experiments, as the increased postural sway with speed is related to increased postural instability which may result in a greater risk for falling [Rogers *et al.*, 2003].

A common method of balance assessment is the use of a moving or servo-controlled platform to disturb balance, such that the balance system can experience environmental uncertainty. This can also be accomplished by using a dense foam pad (sponge) as the support surface [Teasdale *et al.*, 1991]. The center of foot pressure (COP), the center of body mass (COM) and the acceleration profile of a body segment are measured using a portable force mat, a VICON motion capture system and accelerometers, respectively. The equipment used to capture the COM trajectory is expensive and not portable; hence, it is not readily available for a routine clinical assessment. On the other hand, accelerometers are relatively inexpensive and portable, but they do not provide the COM trajectory. However, a recent study [Betker *et al.*, 2006] has shown that the COM can be

estimated from the trunk acceleration during standing with small movements. One of the main objectives of this thesis was to investigate whether the COM during forward stepping can be estimated from the body segments' accelerations.

Feedforward and feedback control systems, such as the human balance control system, have a certain amount of inherent variability [Buzzi *et al.*, 2003]. Even healthy systems possess inherent variability, which allows for adaptation to new environments when disturbances are encountered that affect mobility and postural stability. There are various motor variability measures; trunk acceleration variability was chosen in this research, as the trunk contribution to total body weight is more than any other body segments. Inherent variability present in the human balance control system is not random but deterministic and can be characterized via a nonlinear dynamics descriptor [Buzzi *et al.*, 2003]. In this work, nonlinear dynamic tools were used to extract characteristic features of the COP trajectories during forward stepping. Furthermore, the common linear parameter of postural sway was also investigated for its distinction from the nonlinear parameters.

1.2 OBJECTIVES

- Examining the relationships between the COM trajectory and the body segments' accelerations
- Investigating whether the COM can be estimated from acceleration data
- Investigating motor variability as indicator of human balance control adaptation
- Investigating the characteristics of postural control using linear and nonlinear parameters, namely the sway path length and Rényi dimension of the COP trajectories, respectively

1.3 SCOPE

The remainder of this thesis is subdivided into the following chapters. Chapter 2 provides an outline of the human postural control system and specifies the employed protocols and models. Chapter 3 presents the experimental setup, protocol, data acquisition, and the various modeling systems employed in this thesis. Chapter 4 demonstrates the results for relationship between the COM trajectories and body acceleration, trunk acceleration variability, and of the linear and nonlinear measures of the COP trajectories. Chapter 5 provides a discussion of the results obtained in this thesis. Lastly, Chapter 6 presents conclusions and future work.

CHAPTER 2

HUMAN POSTURAL CONTROL

2.1 POSTURAL CONTROL AND BALANCE

The human body consists of multiple segments. The stability of each body segment is the balance of multiple forces, including gravitational, ground reaction, motion-dependent, and muscle forces [Winter, 1995]. At a global level, a common definition of human balance is the ability to control the position and motion of the centre of body mass (COM) in relation to the base of support (BOS), during tasks such as standing, stepping, walking, and running. Loss of balance occurs when the motion of the COM in relation to the BOS exceeds certain stability limits [Pai *et al.*, 2003]. Our balance is controlled by two neural processes or systems: sensory systems for integrating internal and external referenced spatial information and motor control systems, described in the following subsections.

2.1.1 SENSORY SYSTEMS

The human body depends on various sources of spatial information to define the relationship between internal and external references, with our actions being controlled by feedforward and feedback processes. In terms of sensing the state of balance, spatial information is provided to the integrative centres of the central nervous system (CNS) by visual, vestibular, and somatosensory inputs [Winter, 1995].

As there is some overlap or redundancy in the types of spatial information provided by the various sensory receptors, accurate organization of sensory information is critical

for maintaining balance. Poor sensory integration can lead to impairments in the COM alignment and/or selection of movement strategies and eventually loss of balance [Jeka and Lackner, 1995; Shumway and Cook, 1986].

2.1.1.1 Visual Input

Visual input provides the CNS with the position and motion of one body segment relative to another segment in an internal body reference frame and the position of the body in an external reference frame. However, visually derived motion cues have a relative frame of reference, i.e. the relative information about the motion of the body in its surrounding environment. Thus, visual input may provide inappropriate position and motion cues relative to the actual position and motion of the body, which could initiate a sensory conflict [Peterka, 2002].

2.1.1.2 Vestibular Input

The vestibular sensory system is comprised of two major components: the semi-circular canals which detect angular accelerations and the otolithic organs which detect linear accelerations. Thus, the vestibular sensory system provides the CNS with rotational movements and linear translations, which assist the body in understanding its position relative to the absolute frame of reference [Peterka, 2002].

2.1.1.3 Somatosensory Input

Somatosensory input provides the CNS with the spatial information offered by proprioceptors and exteroceptors, in internal and external reference frames, respectively. Proprioceptors, such as muscle spindles and joint afferents, provide the position and motion of one body segment relative to another. Conversely, exteroceptors, such as

cutaneous (pressure) sensors of the foot, provide the position of the body relative to the ground [Peterka, 2002].

2.1.1.4 SENSORY DEFICIENCY

Many factors can contribute to the degradation of our balance system, including a decrease in sensory information or a deficiency in the central processing of spatial information obtained from the sensory systems, which provide the external and internal reference frames. Early diagnosis and detection of balance impairments are important for management and prevention of functional decline and fall injuries.

The Sensory Organization Test (SOT) is designed to identify deficiencies in a person's use of the sensory systems that contribute to postural control [Nashner, 1971; Peterka and Black, 1990]. The SOT distorts and/or eliminates visual and somatosensory signals through calibrated sway referencing of the support surface and/or visual surrounding. The support surface and the visual surrounding inclinations are synchronized to directly follow the persons's anterior-posterior (A-P) body sway. By controlling the usefulness of the sensory (visual and proprioceptive) information through sway referencing and/or eyes open/closed conditions, the SOT protocol creates a sensory conflict situation by systematically eliminating useful visual and/or support surface information. These conditions isolate vestibular balance control, as well as stress the adaptive responses of the CNS. This evaluates the ability of a person to organize dynamic visual, vestibular, and proprioceptive sensory input into useful information for a stationary standing task.

2.1.2 MOTOR CONTROL SYSTEMS

Human movements are performed in a dynamic environment, where there is a constant change in the demands placed on the CNS to maintain and restore balance or stability during movement. The two control schemes used to regain postural balance are discussed in the following sections.

2.1.2.1 FEEDFORWARD CONTROL

Human upright posture is intrinsically unstable and thus, the main purpose of the CNS is to prevent balance loss that may cause falls or injuries. Balance loss will occur when the instantaneous position and velocity of the COM with respect to the BOS surpass stability limits. The CNS integrates sensory information to examine and revise the current COM state and compares it with the stability limits. Based on prior experience and memory for the COM state, the CNS then performs an appropriate action in a feedforward control manner to oppose perturbation and prevent balance loss [Kuo, 2002; Pai *et al.*, 2003]. Feedforward or predictive control plans the movement beforehand to ensure stability and serves to proactively avoid the destabilizing effect of a disturbance. In this pre-planned scheme, a learning effect improves the capability of predicting disturbances. When these adjustments fail or an unexpected disturbance occurs, the supporting system of feedback control mechanisms plays a role to maintain postural balance [Dietz *et al.*, 1993; Huxham *et al.*, 2001; Schiepatti and Giordano, 2002].

2.1.2.2 FEEDBACK CONTROL

There are many situations where we suddenly lose balance or stumble, i.e. we are caught unawares by an unexpected disturbance. In such situations, timely feedback mechanisms are responsible for rapid corrective balance reactions to restore stability and

prevent falls and/or protective reactions to reduce the risk of fall [Pavol *et al.*, 2002]. Based on the intensity of the perturbation, different feedback control mechanisms may apply to the system. Minor perturbations frequently require the response of an ankle strategy. Stronger perturbations or a narrow support surface may require a hip strategy. Instability or much stronger perturbations may require a step strategy, where the BOS is shifted by taking a step away from the perturbation. These balance strategies are described in detail in Section 2.3. The balance system is believed to satisfy various demands by feedforward control, with feedback control playing an important role in case of unexpected disturbance or unsuccessful feedforward control [Huxham *et al.*, 2001; Kuo, 2002].

2.2 Perturbation Types

The moving platform has been used to examine sensory and motor control processes involved in balance control for nearly four decades. Different velocities, amplitudes [Szturm *et al.*, 1998] and directions [Henry *et al.*, 1998; Carpenter *et al.*, 1999] of the platform translations are used to systematically disturb balance by changing the position of the COM relative to the BOS. Some studies have used platform translations to study the feedforward mechanism, where the platform moves in a sinusoidal fashion; in this case, the timing of the onsets and magnitude of the translations is more predictable.

In [Dietz *et al.*, 1993], sinusoidal platform translations of 0.5, 0.3 and 0.25 Hz, with a constant amplitude of 12 cm, were used to study the feedforward mechanism. The most important finding was the adaptation that took place to the changing frequencies of the translations. When the new platform translation frequency was applied, EMG and biomechanical changes were seen for the next four cycles of the new frequency. Once

this adaptive period was over, there were no significant EMG or biomechanical changes. Hence, after the four adaptive cycles, a feedforward mechanism made prior adjustments before the platform reached the turning point, i.e. the time when the body changed direction from travelling forward to backward or vice versa. A recent study [Schiepatti and Giordano, 2002] demonstrated that an eyes closed condition has an entirely different response than an eyes open condition, during sinusoidal forward and backward platform translation at different oscillation frequencies. Subjects showed two basic modes of coping with the predictable and sinusoidal platform motions, depending on the availability of visual information.

On the other hand, many studies have used the moving platform to characterize and evaluate reactive or feedback controls, where an unexpected perturbation in the form of a sudden platform rotation or translation was applied to the body. When a body is presented with an unexpected perturbation, there are three primary strategies or compensatory reactions employed to maintain balance, depending on the magnitude of the perturbation [Mille *et al.*, 2003]; these strategies are explained in Section 2.3.

In general, platforms can have either a fixed and firm or compliant surface. Each has its own uses and applications. Fixed, predictable, level and firm support surfaces are the most common surfaces used for balance and walking assessment. However, different surface conditions, such as compliant or uneven surfaces typical of outdoor terrains, should also be taken into account to provide a complete assessment. Studies have shown that standing and balancing on a sponge surface can serve as an inexpensive and practical tool to emulate the "sway-stabilizing" conditions of the Sensory Organization Test (NeuroCom International Inc.) [Gill *et al.*, 2001; Teasdale *et al.*, 1991]. Therefore, many

researchers have used a foam pad (sponge) to disturb balance and emulate the uncertainty of outdoor terrain [Cho and Kamen, 1998; Redfern *et al.*, 1997; Runge *et al.*, 1998]. The foam pad introduces uncertainty into the system by distorting and delaying the signals received by the cutaneous sensors and proprioceptors. Due to the distortion and delay, the CNS has difficulty using the centre of foot pressure (COP) as a reference during the balance corrections; hence, it is challenging for the CNS to estimate and determine the necessary adjustments required to control the motion and position of the COM relative to the BOS. Affordability and portability are the advantages of using the foam pad over other methods which use the motorized or servo-controlled platform. Furthermore, different sizes and shapes of foam pads can be obtained to allow various task conditions for standing, stepping and walking. In [Allum *et al.*, 2002], the foam pad's performance was compared to the SOT equipment; the foam pad was found to be a very efficient tool for multi-directional perturbation.

The standing balance of young and older adults using a 5 cm thick foam pad as the support surface was examined in [Teasdale *et al.*, 1991]. The postural sway behaviour of the two groups was examined for 80 seconds under different support surface conditions and with eyes opened/closed. Results showed that the distortion or elimination of one class of sensory input was not sufficient to consistently differentiate between the young and elderly adults; this was due to the fact that the remaining sensory inputs could compensate for the lack of one sensor. However, the combined foam surface and eyes closed conditions had a substantially greater effect on body sway parameters for the elderly, when compared to those of the young adults.

In terms of foot placement accuracy, another important factor in controlling balance is the step velocity. A linear relationship between the approaching velocity and the accuracy of the final foot placement was found in [Bradshaw and Sparrow, 2001], where the effects of the approaching velocity were studied during walking, jogging and sprinting towards an obstacle along a 10 m walkway. It was shown that the increased postural sway with speed was related the increased postural instability, which may result in a greater risk of falling [Rogers *et al.*, 2003]; hence, it is important to consider the velocity in stepping or walking experiments.

2.3 Balance Strategies

The response to a disturbance is determined by the type, direction and nature of the perturbation. Depending upon the degree of the perturbation, the reaction could be either an in-place response or a stepping strategy. In minor perturbations of slow and small amplitudes, generally an in-place strategy (ankle or hip strategy) is used, while in faster and larger amplitude perturbations, a stepping strategy is used [Maki *et al.*, 1996; Pavol and Pai, 2002].

2.3.1 Ankle Strategy

Slow and minor perturbations lead to an ankle strategy, where the body acts as an inverted pendulum with the ankle acting as the pivot point. As the movement of an inverted pendulum is completely rigid with no breaks in the long segment, the lower limbs and the trunk move in the same direction. The movement primarily takes place around the ankle joint [Nashner, 1976; Diener *et al.*, 1988; Horak *et al.*, 1989].

2.3.2 HIP STRATEGY

For medium degrees of disturbances, a hip strategy is observed to maintain balance. In this strategy, the body breaks up into a dual segment pendulum, with the head and trunk comprising one segment and the lower limbs comprising the second. This strategy involves plantar flexion movement around the ankle, causing the shank to move backwards, and a flexion at the hip and trunk. Here the trunk counters the lower body as the COM needs to be moved to a stable position [Runge *et al.*, 1999; Ko *et al.*, 2001].

2.3.3 STEPPING STRATEGY

Another type of balance reaction, which is observed in response to a large perturbation, is a stepping strategy. If the person is destabilized beyond the limits of in-place strategies (ankle or hip strategy), he/she depends on the stepping strategy. Instead of keeping the feet stationary, the person takes a quick step to move the BOS to encompass the predicted COM position. In [Maki *et al.*, 1996], different directions and magnitudes of perturbation were used to study how a perturbation affects the swing leg selection and temporal characteristics of the swing trajectory. For large perturbations, the possible ways to move the foot in a stepping reaction are: to take a small step with the loaded leg, to take a step with the unloaded side, or to take multiple steps. Taking a step with the unloaded side requires one to take the step across the body, i.e. relocate the BOS towards the COM, which is moving in the opposite direction.

2.4 COM AND ITS RELATIONSHIP WITH BODY SEGMENTS' ACCELERATIONS

Good balance during stepping and walking is important to avoid falls causing injuries. The need for good balance becomes more pronounced when walking outdoors, where unexpected conditions, disturbances, and stumbles are inevitable. Stumbles and falls will

occur if the COM moves outside the BOS or has insufficient momentum to re-enter the BOS. This is especially important during stepping where there is a single limb support phase. The COM trajectory is often used as a key index of both mobility and balance during stepping and walking; it is an important measure of stability in modeling the human postural control system.

Currently the COM trajectories are computed by force plate and/or motion analysis systems, which consist of reflective markers, infrared LED cameras and a motion processing workstation. The system is very expensive and not portable and is thus unavailable for a routine clinical assessment. A more affordable and portable system is required for a routine clinical assessment. Several models were developed to estimate the COM trajectories during standing [Chan, 1999; Barbier *et al.*, 2003; Lapond *et al.*, 2004]. In [Chan, 1999], an approach for obtaining the COM from force plate data was introduced; the horizontal COM position was obtained by double integrating the horizontal ground reaction forces. An average correlation of 0.903 with a standard deviation 0.091 was found. In [Barbier *et al.*, 2003], force plate data was used to compute the COM trajectory using an inverted pendulum model and the results were compared with the actual COM trajectory obtained from a video motion capture system. Their model estimated the COM trajectories within a root mean square (RMS) difference of 0.9 mm and the correlation coefficients between the model and the video method were above 0.8 in both the A-P and medial-lateral (M-L) directions. In [Lapond *et al.*, 2004], three methods were compared, which estimated the COM using a force plate and a 3-D kinematic system; the methods were: a) the kinematic model, b) the double integration technique (GLP), and c) the COP low-pass filter method (LPF). They considered four

different standing tasks: a) quiet standing, b) one leg standing, c) voluntary oscillation about the ankles, and d) voluntary oscillation about the ankles and hips. The GLP and LPF models estimated the COM trajectories during quiet standing within a RMS difference of 1.0 mm in both A-P and M-L direction.

The force plate and video motion capture systems required to study the COM trajectory in the aforementioned studies are expensive and not portable and thus, the techniques are unavailable for a routine clinical assessment. On the other hand, accelerometers are inexpensive and portable; however, they do not provide the COM trajectory.

In [Wu and Ladin, 1996], the 3-D kinematics of the human lower limb during walking and running was studied, in order to examine the relative contribution of linear acceleration measurements. The position, angular velocity, and linear acceleration of the foot, shank, and thigh segments were measured to examine the segmental COM estimates. It was found that the angular velocity and linear acceleration measurements can increase the accuracy of COM estimates. This study suggests that the COM trajectory may be successfully estimated by acceleration measurements of lower limb segments.

A recent study [Betker *et al.*, 2006] showed that the COM trajectories could be estimated using accelerometer data. Three models (neural network, adaptive fuzzy and genetic sum-of-sines) were introduced to estimate the resultant COM trajectory using trunk acceleration data, during standing with the hip strategy. Among the three models, the genetic algorithm sum-of-sines model had superior performance and provided an estimate of the resultant COM trajectory within an average error of 10%. This is an

encouraging result for integrating the COM estimation models with a clinical assessment system.

Some studies [Chan, 1999; Barbier *et al.*, 2006; Lapond *et al.*, 2004] have attempted to examine the COM trajectory during standing; however, there is little research studying how the COM relates to body segment accelerations during forward stepping. The kinematics of forward stepping is quite different from that of standing; the M-L relocation of body weight support is functionally required for stepping, whereas the M-L COM is usually positioned around the centre above the BOS between the feet during stationary standing [Rogers *et al.*, 2001]. In addition, when the swing foot is lifted for a stepping procedure, the BOS is remarkably reduced to the area of the singly supported foot. Body corrections are required in order to keep the body from falling towards the swing foot. In order to reduce the possibility of falling laterally at the time of the foot lift, the COM should be pushed toward the single supported side [Rogers *et al.*, 2001]. Thus it is useful to study balance control during forward stepping during different task conditions prior to investigating steady state walking.

2.5 Trunk Acceleration Variability

When compensating for any perturbation to retain stability, inherent motor variability exists [Buzzi *et al.*, 2003]. Increases in variability have been shown in less stable systems, e.g. elderly with a history of frequent falls; hence, gait variability may provide an indication of the lack of adaptability [Newell and Corcos, 1993]. Measures of gait variability, such as variability in step length, step width, speed, stance time and swing time, have been examined as feasible indicators of balance control by many researchers [Hausdorff *et al.*, 1997; Maki, 1997; Gabell and Nayak, 1984; Sekiya *et al.*, 1997;

Grabiner *et al.*, 2001; Stolze *et al.*, 2000]. As the trunk contributes to the total body weight more than any other body segment, measures of variability regarding movements of the trunk have been studied. [Moe-Nilssen and Helbostad, 2005] examined step width variability and trunk acceleration variability in fit people and frail elderly, investigating how the parameters distinguish between the two groups. Step width variability was measured from footprints and trunk acceleration variability was measured by an unbiased autocorrelation procedure. Their results showed that trunk acceleration variability classified 80% of the subjects correctly into their group, while step width variability did not differ between groups.

2.6 CHARACTERISTICS OF THE COP

Instability will occur if the COM moves out of the BOS or if it has insufficient momentum to regain the BOS. The COP is a useful indicator of this instability, as its trajectory represents the balance reaction in both the frontal and sagittal planes [Shan *et al.*, 2004; Szturm and Fallang, 1998; Collins and De Luca, 1993; Gatev *et al.*, 1999]. It is implicitly assumed that the postural sway indexed by the COP is a stationary process. In addition, most studies have limited the analysis of the COP trajectory to standard statistics. However the assumption of stationarity does not hold in all situations. Studies have shown that many physiological systems (including postural sway) are chaotic [Doyle *et al.*, 2004; Yamada, 1995; Błaszczyk and W. Klonowski, 2001; Buzzi *et al.*, 2003; Hausdorff *et al.*, 2001]. Recent studies have developed analysis tools to evaluate nonlinear and chaotic properties of the postural control systems [Doyle *et al.*, 2004]. As suggested in [Buzzi *et al.*, 2003], feedforward and feedback control systems have a certain amount of inherent variability, which is not random but deterministic, and can be

characterized via nonlinear descriptors. Another study demonstrated that the COP trajectories are chaotic [Yamada, 1995]. Fractal analysis of stride-to-stride fluctuations in human gait rhythm was performed in [Hausdorff *et al.*, 2001]; it was found that a fractal pattern is present in stride fluctuations of healthy subjects during walking. Fractal analysis of the COP trajectories using Higuchi's algorithm [Higuchi, 1988] was performed in [Błaszczyk and W. Klonowski, 2001]. A difference between the tasks was found, when the subjects stood still on a firm surface with eyes open and closed. The results of these studies encourage the use of nonlinear dynamics in describing and understanding variability and subsequently, in identifying balance disorder status. The characteristics of postural control were investigated using COP sway path and nonlinear parameters. The significance of nonlinear analysis to describe system characteristics as a function of different task conditions and the advantage of nonlinear tools over linear parameters are discussed.

CHAPTER 3

METHODOLOGY

This chapter discusses the experimental design, the models describing the relationship between the body accelerations and COM, and the nonlinear analysis of the COP trajectories in comparison with linear analysis. The relationship between the COM trajectories and the body accelerations was investigated through a fuzzy inference model, a sum-of-sines model, and a parabolic model. The nonlinear characteristics of the COP trajectories were evaluated using the Rényi dimension and spectrum, which were then compared to the linear sway path used as linear parameter.

3.1 EXPERIMENTAL DESIGN

3.1.1 SUBJECTS

Nineteen young healthy subjects (aged 26.5 ± 2.22, 9 females) with no history of neurological disorder or postural problems volunteered to participate in this study. Prior to recruiting subjects, ethics approval was granted by the Ethics Committee, Faculty of Medicine, the University of Manitoba. All subjects gave informed consent and were briefed about the tasks and instrumentations before the experiments. Body indexes of participating subjects, such as weight, height and Body Mass Index (BMI), of participating subjects are given in Table 3.1; which provides the mean, standard deviation, minimum, and maximum values for each body index is also given.

Table 3.1 Averaged index of subjects.

Index	Mean ± SD	Minimum	Maximum
Height (m)	1.69 ± 0.10	1.56	1.90
Weight (kg)	67.01 ± 14.15	47	96
BMI (kg/m^2)	23.09 ± 2.82	18.36	28.05

3.1.2 Experimental Setup

Two different 10 cm thick foam pads were used to emulate the uncertainty of outdoor terrain: No. 1 was of dimension 50.8 × 50.8 cm with a 25% indentation force deflection of 62.64 kg and No. 2 was of dimension 50.8 × 50.8 cm with a 25% indentation force deflection of 31.82 kg. A 2 cm thick wooden board of dimension 25.4 × 40.64 cm was placed on top of the foam pad in order to equally distribute the forces applied by the body on the foam pad, which minimizes the effect of differences in body weight.

Vertical pressure forces were recorded with a thin flexible Force Sensing Application (FSA) mat (Vista Medical Ltd., Winnipeg, MB, Canada) that was placed on top of the foam pad. This 0.036 cm thick pressure mat of dimension 53 × 53 cm consists of a 32 by 16 grid of piezo resistive sensors spaced 2.8575 cm apart, which were sampled at a frequency of 25 Hz. The vertical COP in the A-P and M-L planes was then calculated as the spatial centre of all the forces for the given mat.

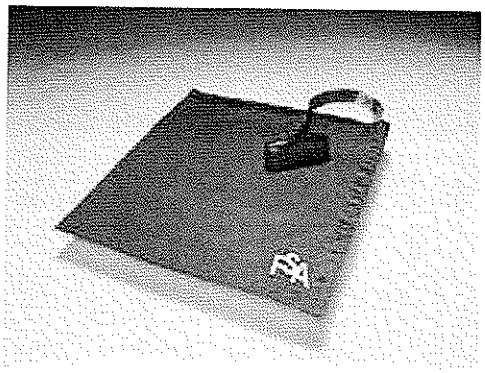

Figure 3.1 Force Sensing Application (FSA) mat

A VICON 460 motion capture system (Vicon Peak, Centennial, CO, USA) was utilized for the whole body motion analysis. A total of 31 reflective markers were placed on the subject's anatomical positions representing whole body segments. Appendix A depicts the detail of marker positions employed in this study. Six infrared LED cameras captured 3-D motions, which the VICON motion capture system then processed to provide kinematic data including segment positions, segment angles and the COM. The sampling frequency was 120 Hz. As the VICON motion capture system is not equipped with a trigger input channel, a custom circuit was designed to trigger it using the trigger output from the FSA mat's module box.

Figure 3.2 VICON motion capture system

Three miniature tri-axial S2-10G-MF accelerometers (Biometrics Ltd., Ladysmith, VA, USA) of dimensions 2 × 1 × 1 cm and weight of 30 g were utilized to record segment movement. They were placed on the subject's upper trunk close to the T2 vertebra, the shank of the stance leg, and the lateral malleolus of the swing leg. A total of

9 analogue signals (A-P, M-L and vertical directions for each accelerometer) were digitized using the A/D converter card built into the VICON motion capture system; a custom interfacing panel was employed to bridge between the analogue devices and the VICON patch panel. The sampling frequency was 1080 Hz, as set by the manufacturer.

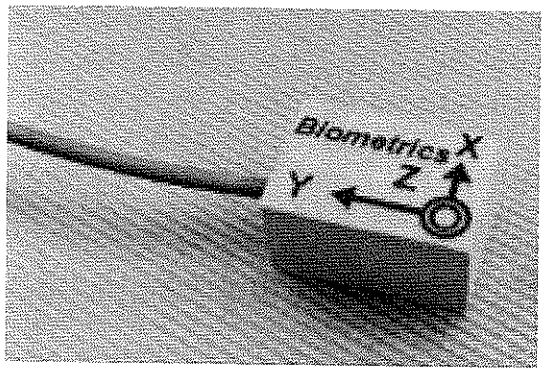

Figure 3.3 Biometrics S2-10G-MF accelerometer

3.1.3 PROTOCOL

Subjects were instructed to stand with their feet parallel, approximately 10 cm apart on the fixed level firm surface. Next, they took a forward step with their right leg at a normal self-paced speed and came to a complete stop for five seconds. They then brought their swing leg back to the starting position in order to get prepared for the next forward step. During backward stepping, they were allowed to look down to make sure their right foot returned to the correct starting position as marked on the FSA pressure mat. Once the subjects were set at the correct starting position, they were instructed to take another forward step. This process was repeated until the number of forward steps listed in Table 3.1 was taken for each trial. For the next trial, subjects were instructed to take 10 forward steps at a slow speed. Both of these stepping tasks were repeated on foam pad No. 2. However, only the self-paced speed trial was performed on foam pad No. 1. A rest period was given between each trial in order to prevent any factor resulting

from fatigue. A few practice steps were performed prior to each trial. To prevent subjects from becoming fatigued, the total time of each experiment is supposed to should be less than an hour. Due to this restriction, some trials were set to 10 forward steps instead of 20. Table 3.2 lists the number of forward steps performed by a subject during each trial.

Table 3.2 Number of Forward Steps Performed by a Subject.

Trial	Number of Forward Steps
Fixed Surface, Normal Speed	20
Fixed Surface, Slow Speed	10
Foam Pad 1, Normal Speed	10
Foam Pad 2, Normal Speed	20
Foam Pad 2, Slow Speed	10

3.1.4 PRE-PROCESSING

The total number of stepping data collected in this study was 133, i.e. seven per subject. The trunk and swing acceleration data was decimated to a sampling rate of 120 Hz, which was that of the kinematic data. In order to account for physical differences between the subjects, the data was normalized by subtracting the mean, and dividing by the absolute maximum value. The COM trajectory computed by the VICON motion capture system was found to be incomplete in a few trials; hence, those trials were excluded from the COM estimation (Table 3.3). The vertical position of the ankle marker was used to detect and extract the forward stepping phase, from swing foot lift to heel strike.

Table 3.3 Number of Incomplete Trials.

Trial	Number of Incomplete Trial
Fixed Surface / Normal Speed*	2 / 38
Fixed Surface / Slow Speed	0 / 19
Foam Pad 1 / Normal Speed	0 / 19
Foam Pad 2 / Normal Speed*	1 / 38
Foam Pad 2 / Slow Speed	1 / 19
Total	4 / 133

Note: The trials that subjects performed 20 forward steps are marked with an asterisk (*).

3.2 Modeling Procedure

This section describes: (a) the application of three different models (fuzzy inference model, sum-of-sines model, and parabolic model) to investigate the relationship between the COM trajectories and the body accelerations, plus a genetic algorithm was used to update the model coefficients; (b) the application of trunk acceleration variability to examine whether inherent motor variability exists in the system; and (c) the application of nonlinear dynamics (Rényi dimension and spectrum) and a linear parameter (sway path) to study the characteristics of the COP trajectory.

3.2.1 Adaptive Network-Based Fuzzy Inference System

A classical set is a set that totally includes or excludes any element. In this set, the boundary is so strict that an element must be in either set X or set not–X. However, there are many occasions that this Boolean logic is not helpful, i.e. an element can be in multiple sets. In such occasions, a fuzzy set is useful, as reasoning in fuzzy logic allows for a generalization of the Boolean logic. For example, if the numerical value of 1 is given to true and the numerical value of 0 is given to false, fuzzy logic allows in-between values such as 0.25 and 0.847. A fuzzy inference system expresses the mapping from

input to output using fuzzy logic. The mapping provides a source to make a decision. The process of fuzzy inference involves membership functions, logical operations and if-then rules, which qualitatively develop the characteristics of conceptual knowledge and interpret processes without precise quantitative analysis.

A membership function classifies how each input point is mapped to a degree of membership between 0 and 1. The possibility of partial membership in a fuzzy set is admitted. The membership function can be common functions, such as the piece-wise linear function, the Gaussian distribution function, the sigmoid function, and the trapezoidal function, or custom functions. Logical operations in fuzzy logic include a standard truth table, such as AND, OR and NOT; however, the input values in fuzzy logic can be a real number between 0 and 1. Thus, an AND truth table is defined by the minimum operator, an OR by the maximum operator, and a NOT by the $1 - \{Input\}$ operation. The if-then rules are used to formulate the conditional statements containing fuzzy logic. An if-then rule consists of three distinct parts: a) fuzzifying the input, b) applying the necessary fuzzy operators, and c) applying the results to the implication. Finally, the resulting set is defuzzified to a single value. In the case where the if-then rules of the system are known, they are used to define the membership functions. However, if the if-then rules are unknown, the if-then statements can be obtained by adaptively revising the parameters of the membership functions as described in [Jang, 1993].

The values of each input membership function are determined during the fuzzification. The weight coefficient w_R of each if-then rule is determined based on

$$w_R = \prod_{i=1}^{I} \Lambda_{Ri} , \tag{3.1}$$

where Λ is the value of the input membership function. The normalized weight is then computed based on

$$\overline{w}_i = \frac{w_i}{\sum_{k=1}^{N_R} w_k}, \tag{3.2}$$

where N_R is the number of if-then rules, and it is obtained by

$$N_R = \prod_{k=1}^{I} N_k , \tag{3.3}$$

where I is the total number of inputs, and N_k is the number of input membership functions for the input. The value of each output membership function f_i is determined as a function of w_i. During defuzzification, the output of the system $\hat{F}$ is defined as

$$\hat{F} = \sum_{i=1}^{N_R} \overline{w}_i f_i . \tag{3.4}$$

Then the membership function parameters can then be updated to adaptively optimize the model.

There are two fuzzy inference methods: Mamdani-type and Sugeno-type. Mamdani-type is the most commonly used fuzzy technique and is the fuzzy inference process that has been described. The Sugeno-type fuzzy inference method is similar to the Mamdani-type method; the first two parts of the fuzzy inference process, a) fuzzifying the inputs and b) applying the fuzzy operator, are the same. The only difference is that the output membership functions are linear or constant for the Sugeno-type method.

The Fuzzy logic toolbox along with custom scripts in MATLAB 7.0 Release 14 (MathWorks, Natick, MA, USA) was used. The inputs to the model were trunk and swing leg accelerations, in the A-P and M-L directions. A generalized bell-shaped membership function was selected through trial and error; the number of membership

functions assigned to each input was 8, the number for which the system showed the best performance. The number of epochs was set to 20 through trial and error. The model was trained for each trial according to the leave-one-out procedure. The Sugeno-type method was used for the fuzzy inference and a linear function was selected for the output membership function; and these were set by the fuzzy logic toolbox.

3.2.2 SUM-OF-SINES MODEL

A sum of sinusoidal harmonics can be used to approximate a target function

$$d(t) = a_0 + \sum_{n=1}^{H} a_n \sin(n\omega_0 t + \theta_n), \tag{3.5}$$

where H is the number of harmonics, a are amplitude coefficients, w_0 is the fundamental frequency on which the harmonics are based, t is time and θ represent phase shifts [Winter, 1995]. In order to find the COM as a function of an input signal, not as a function of time, the sum of sines model in (3.7) can be modified as follows:

$$\hat{COM}(X) = \sum_{n=1}^{H} a_n \sin(f_n X + \theta_n), \tag{3.6}$$

where $\hat{COM}(X)$ is the estimated COM as a function of the signal X [Betker et al., 2006]. Parameters H, a, θ and f will be determined by the genetic algorithm.

3.2.3 PARABOLIC MODEL

Forward step data was extracted from the actual COM and acceleration signals. Preliminary investigation of the relationship between the acceleration signals and COM suggested a parabolic model as the best fit as depicted in Figure 3.1. For a parabola opening to the right with a vertex at (X_0, COM_0), the equation in Cartesian coordinate is

$$(COM - COM_0)^2 = a(X - X_0), \tag{3.7}$$

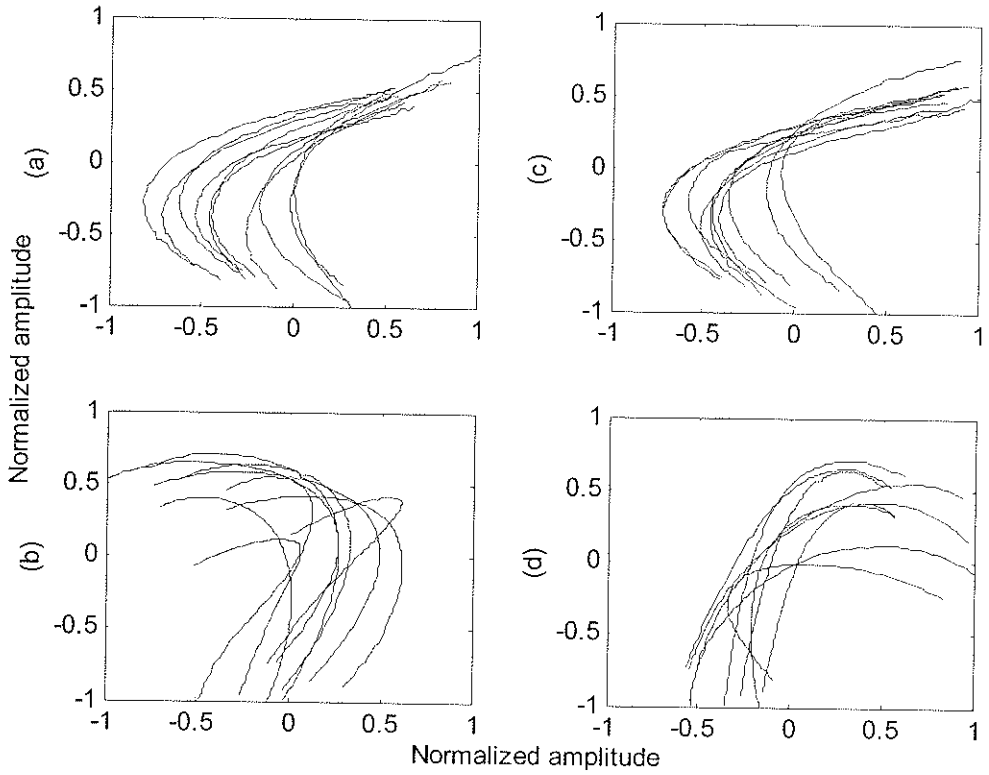

Figure 3.4 Relationship between the COM and swing leg acceleration for a typical subject in (a) A-P direction and (b) M-L direction; the relationship between the COM and trunk acceleration for a typical subject in (c) A-P direction and (d) M-L direction.

where X is the independent variable and a is the latus rectum (the chord through a focus parallel to the conic section directrix) [Coxeter, 1969]. Employing equation (3.7) for the COM estimation from acceleration data, the following equation was used to estimate the A-P and M-L components of the COM from trunk and swing acceleration:

$$\hat{COM}_j(X_{ij}) = \pm a_{ij}\sqrt{X_{ij} - X_{ij_0}} + b_{ij}, \tag{3.8}$$

where X_{ij} is body acceleration, a_{ij} and b_{ij} are the parameters to be estimated, the subscript i represents trunk acceleration when $i = 1$ and swing leg acceleration when $i = 2$, and the subscript j represents the A-P direction when $j = 1$ and the M-L direction when $j = 2$.

Due to the geometry of a typical parabola opening to the right, X_{ij0} can be estimated as the minimum value of the independent variable. Then equation (3.8) becomes

$$\hat{COM}_j(X_{ij}) = \pm a_{ij}\sqrt{X_{ij} - \min(X_{ij})} + b_{ij}. \tag{3.9}$$

A linear combination of two parabolic equations, i.e. trunk and swing leg acceleration, was chosen to form the final relationship through a trial and error procedure. The estimated COM is then

$$\begin{aligned}\hat{COM}_j(X_{1j}, X_{2j}) = a'_{1j}\hat{COM}_j(X_{1j}) \\ + a'_{2j}\hat{COM}_j(X_{2j}) + b'_j,\end{aligned} \tag{3.10}$$

where a'_{1j} and a'_{2j} are the updated coefficients of a_{1j} and a_{2j}, respectively, and b'_j is equal to $b_{1j} + b_{2j}$. The model parameters were estimated using two techniques: a genetic algorithm and simulated annealing. Data from all subjects except one was used to calibrate the model and the left-out data was used to test the performance of the model. This leave-one-out procedure was repeated until every subject's data was used for testing.

3.2.4 GENETIC ALGORITHM

A genetic algorithm is a stochastic global search method that imitates the natural evolution process. It applies the survival of the fittest strategy to improve a set of parameters for optimization and create a better approximation to a solution [Chipperfield *et al.*, v 1.2]. Genetic algorithm terminology includes gene (the basic building block, representing variables), chromosome (string of genes), individuals (current or candidate solutions), population (array of individuals), generation (each successive population), parents (selected individuals in the current population), children (created individuals in the next generation), fitness function (the objective function to optimize), and fitness

value (the value of the fitness function for an individual). Individuals in the population are encoded as chromosomes to map the problem domain onto the decision domain. For the purpose of mapping, the encoding type, upper and lower bounds, and precision should be selected. The most common representation type for chromosomes is a binary string of 0s or 1s; however, there are various representation types, such as real value, alphabet or Grey code. The number of bits required b should satisfy the relationship

$$L \cdot 10^{p} < E^{b}, \tag{3.11}$$

where L is the length of the parameter calculated as $L = UB - LB$, where UB is the upper bound, and LB is the lower bound, p is the precision and E is the base of the encoding type [Michalewicz, 1996]. The chromosome is defined as a combination of the encoded genes, and then a population of n individuals is randomly generated. In each generation, N new individuals will be created according to the relationship

$$N = \lfloor P \cdot G \rfloor, \tag{3.12}$$

where P is the number of individuals in the population and G is the generation gap [Michalewicz, 1996]. The fitness value is then calculated for each individual in the population.

The following steps are repeated for each generation until a stop criterion is satisfied: 1) select individuals to reproduce, based on their fitness values; 2) apply genetic algorithm operations, such as crossover and mutation; 3) evaluate the fitness function for each individual in the new generation,; and 4) insert fit individuals into the current population to replace less fit individuals. In the first step, a fitness value that suggests the degree of achievement is assigned to each individual by the fitness function. Individuals that will be used for reproduction are selected from the population according to their

fitness values. Selection methods include roulette wheel selection, rank selection, tournament selection, local selection and truncation selection. In the second step, the individuals selected reproduce to create new individuals by means of genetic operations, such as crossover and mutation. Crossover occurs with the probability P_c and involves random selection of crossover points. The children produced by the crossover share the characteristics of their parents. Mutation alters randomly chosen mutation points of the children resulting from the crossover with a given probability

$$P_m = \frac{0.7}{L_c}, \tag{3.13}$$

where L_c is the length of the chromosome [Michalewicz, 1996]. In the third step, the fitness value is obtained for each individual that was reproduced by the genetic operations. In the last step, less fit individuals in the current population are replaced by more fit individuals. The selection of individuals for insertion into the new generation is based on their fitness values.

The genetic algorithm toolbox [Chipperfield *et al.*, v 1.2] with custom scripts in MATLAB 7.0 Release 14 (MathWorks, Natick, MA, USA) was used. The encoding type was Grey code with the base of the encoding type E was= 2, and the lower bound LB and upper bound UB were defined as [-1, 1], with a precision p of 4; and these were chosen through trial and error. Thus, a number of bits b of 15 was required to encode the parameters according to the criterion (3.4). A generation gap G of 0.9 was used, and the fitness function used in this thesis was the mean square error (MSE)

$$MSE = \frac{1}{M}\sum_{i=1}^{M}\left(COM_i - \hat{COM}_i\right)^2, \tag{3.14}$$

where M is the length of the signal, COM is the actual COM trajectory and $\hat{COM}$ is the estimated COM trajectory. The fitness function executes a linear ranking, based on minimizing the MSE. The fitness value is

$$F_j = \frac{S}{P-1} i \cdot MSE_j \qquad i = P-1,\ldots,0, \tag{3.15}$$

where S is the selective pressure, j is the original position of the individuals in the population before ordering, and MSE_j is the sorted MSE in ascending order at the j^{th} position [Chipperfield *et al.*, v 1.2]. A maximum generation number of 100 was chosen through trial and error, and was used as the stopping criterion for training. The method used to select individuals for reproduction was stochastic universal sampling (SUS). In this method, each individual is mapped onto a segment of a line, such that each individual's segment is equal in size to its fitness value. The distance between N pointers is $1/N$ and the first pointer p_0 is randomly generated between

$$\left[0, \frac{1}{N} \cdot \sum_{i=1}^{P} F_i\right], \tag{3.16}$$

while the rest of pointers are generated according to

$$p_i = p_0 + \frac{i}{N} \qquad i = 1\ldots, N-1. \tag{3.17}$$

When the pointer value exceeds the sum of the fitness values, it proceeds to the next available line segment on the far left side so that all pointer values lie on a line. The individuals whose fitness values land at a pointer are selected to reproduce. The A crossover probability P_c of 0.85, and a mutation probability P_m of 0.088, computed from equation (3.13), were used.

The estimation error between the target and estimated COM trajectories was computed by

$$e = \frac{\hat{COM} - COM}{COM} \cdot 100\%, \tag{3.18}$$

where $\hat{COM}$ and COM are the estimated and actual COM trajectories, respectively. This error calculation was applied to all models. The mean and standard deviation of the estimation error for each subject during each task condition was then calculated.

3.2.5 Trunk Acceleration Variability

Trunk acceleration variability was measured using the amount of the correlation coefficient at the first dominant peak of the trunk acceleration's autocorrelation sequence of the trunk acceleration. The period from zero to the first dominant peak of the trunk acceleration autocorrelation sequence represents the phase shift equal to one step [Moe-Nilssen and Helbostad, 2005]. The trunk acceleration variability from stride to stride may be reflective of the specific motor control used to maintain the balance [Moe-Nilssen and Helbostad, 2005]. Hence, in this study trunk acceleration variability was calculated in both the M-L and A-P directions for all experiments and; the results were investigated for any correlation with the COM modeling error. The mean and standard deviation of trunk acceleration variability was then calculated among the subjects.

3.2.6 Characteristics of the COP

3.2.6.1 Rényi Dimension and Spectrum

The information dimension and correlation dimension are special cases related to the generalized entropy concept, as introduced by mathematician Alfréd Rényi in 1955 [Kinsner, 2004]. Rényi generalized the entropy to any moment order q as

$$H_q = \frac{1}{1-q}\log\sum_{j=1}^{N_r} p_j^q \qquad 0 \le q \le \infty, \tag{3.19}$$

where H_q is the entropy at moment order q and p_j^q is the probability (relative frequency) of the j^{th} volume element at moment order q. If we assume a power-law relationship as follows

$$\left(\sum_{j=1}^{N_r} p_j^q\right)^{\left(\frac{1}{1-q}\right)} \sim \frac{1}{r}^{D_q}, \tag{3.20}$$

then the Rényi dimension spectrum D_q is

$$D_q = \lim_{k\to\infty}\frac{1}{q-1}\frac{\log\sum_{j=1}^{N_k}\left(p_j^q\right)}{\log\left(r_k\right)}. \tag{3.21}$$

The Rényi dimension is called the similarity dimension D_S when q=0, the information dimension D_I when q=1, and the correlation dimension D_C when q=2. Using the algorithm presented in [Kinsner, 2004] for entropy-based dimensions, the Rényi dimension at moment order q from 0 to 9 was calculated, which was designed for use with time series data such as the COP trajectory. Prior to applying the algorithm to real data, the algorithm was verified using well-known fractals, such as Koch and Minkowski curves simulated by executing L-system. The results showed that the algorithm was able to explain up to 90% of the theoretical fractal dimensions of the Koch and Minkowski curves.

Due to its concept of generalization, the Rényi dimension D_q can present the fractal dimension at any moment order q. By combining the Rényi dimensions at different moment orders, one can construct the Rényi spectrum as a function of moment order q. The Renyi spectra calculated from the COP trajectories were investigated for

any possible different pattern differences between task conditions, i.e. support surface or stepping speed.

3.2.6.2 SWAP PATH LENGTH

The sway path length, *SP*, is known as a linear clinical parameter that provides an indication of the amount of the postural activity. As the following equation shows, the sway path length presents the sum of the Euclidean distance between two sample points in the COP trajectory, divided by the duration of measurement *dT*.

$$SP = \frac{\sum_{n=1}^{N-1} \sqrt{\left(COP_{n+1}^{AP} - COP_{n}^{AP}\right)^2 + \left(COP_{n+1}^{ML} - COP_{n}^{ML}\right)^2}}{dT} \tag{3.22}$$

As the sway path length provides a direct indication of the amount of the posturographic activity, it was shown as one of the most valuable clinical parameters in the analysis of human postural control for a variety of conditions [Baratto *et al.*, 2002]. In this thesis, the sway path length was represented as a valid linear parameter of postural activity; it will be compared it with nonlinear parameters, specifically the Rényi dimension, to investigate whether there is any significant difference between them and/or any advantage of utilizing nonlinear parameters over the linear ones.

CHAPTER 4

RESULTS

4.1 COM IN RELATION TO ACCELERATION

Figure 4.1 depicts the body accelerations of the trunk and swing leg, along with the corresponding COM trajectory, of a forward step performed for two different tasks, for a typical subject: 1) fixed surface at a normal speed; and 2) foam pad No. 2 at a slow speed.

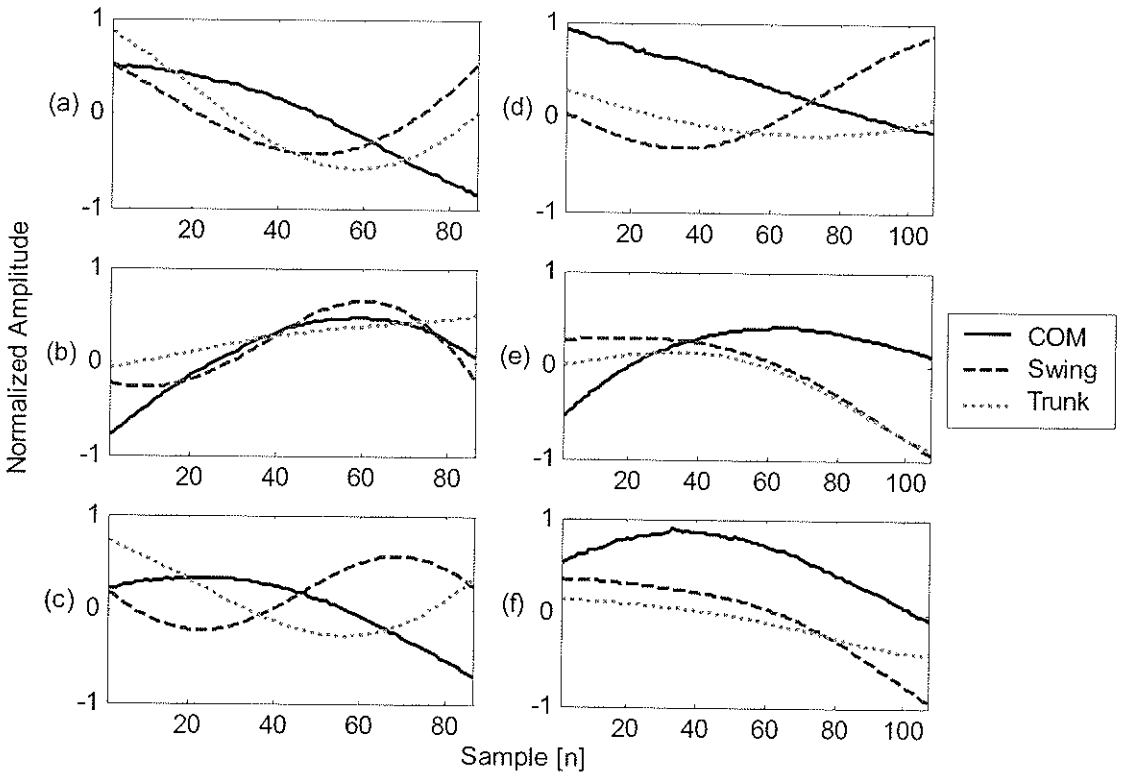

Figure 4.1 COM, swing leg acceleration and trunk acceleration for a typical subject performed on: a fixed surface at a normal speed in (a) A-P direction, (b) M-L direction and (c) resultant; and foam pad No. 2 at a slow speed in (d) A-P direction, (e) M-L direction and (f) resultant. One forward step is shown in the figure.

The subsequent sections present the results for the adaptive fuzzy inference model, genetic algorithm sum-of-sines model, and genetic algorithm parabolic model, respectively.

4.1.1 Adaptive Fuzzy Inference Model

An adaptive fuzzy inference model was trained and tested for each of the seven stepping trials. The results for a typical subject for the task condition on a firm surface at a normal speed in the A-P direction, M-L direction, and the resultant trajectory are shown in Figure 4.2. The results for a typical subject for the task condition on foam pad No. 2 at a slow speed in the A-P direction, M-L direction, and the resultant trajectory are shown in Figure 4.3.

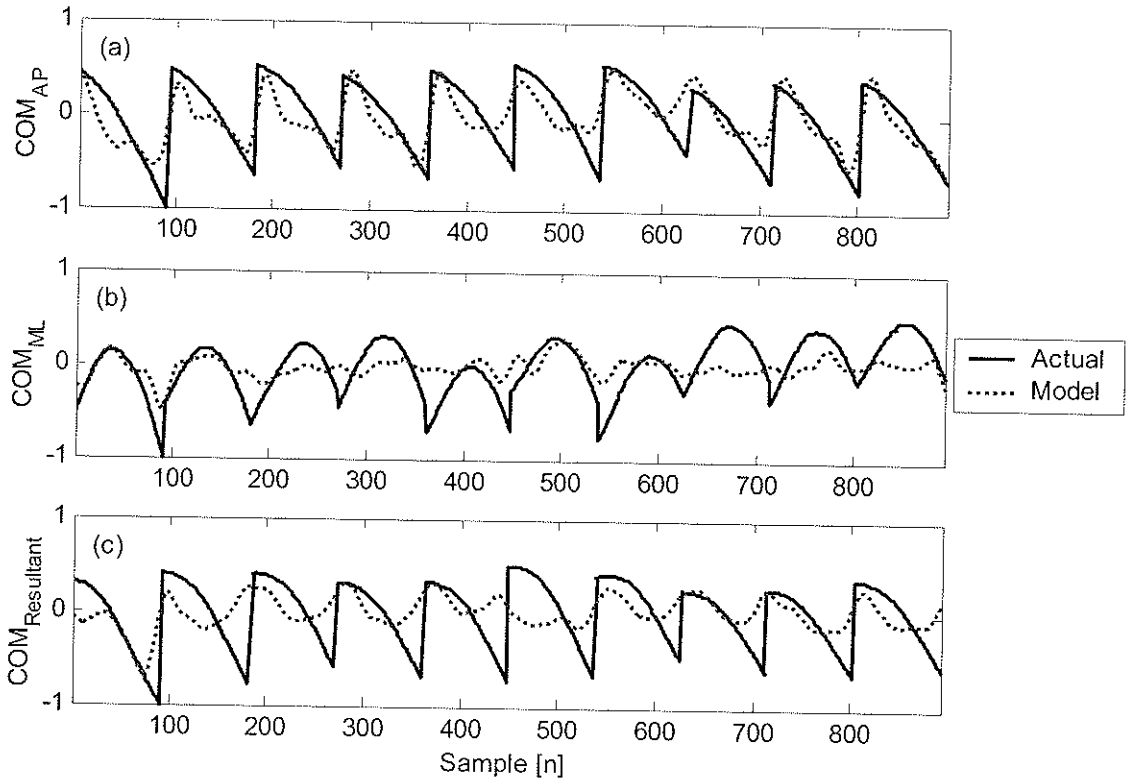

Figure 4.2 Adaptive fuzzy inference model results: normalized actual and developed COM trajectories in (a) A-P direction, (b) M-L direction, and (c) resultant for a typical subject for the stepping task on a fixed surface at a normal speed. For display purposes, the end point of the previous forward step is connected to the start point of the next forward step.

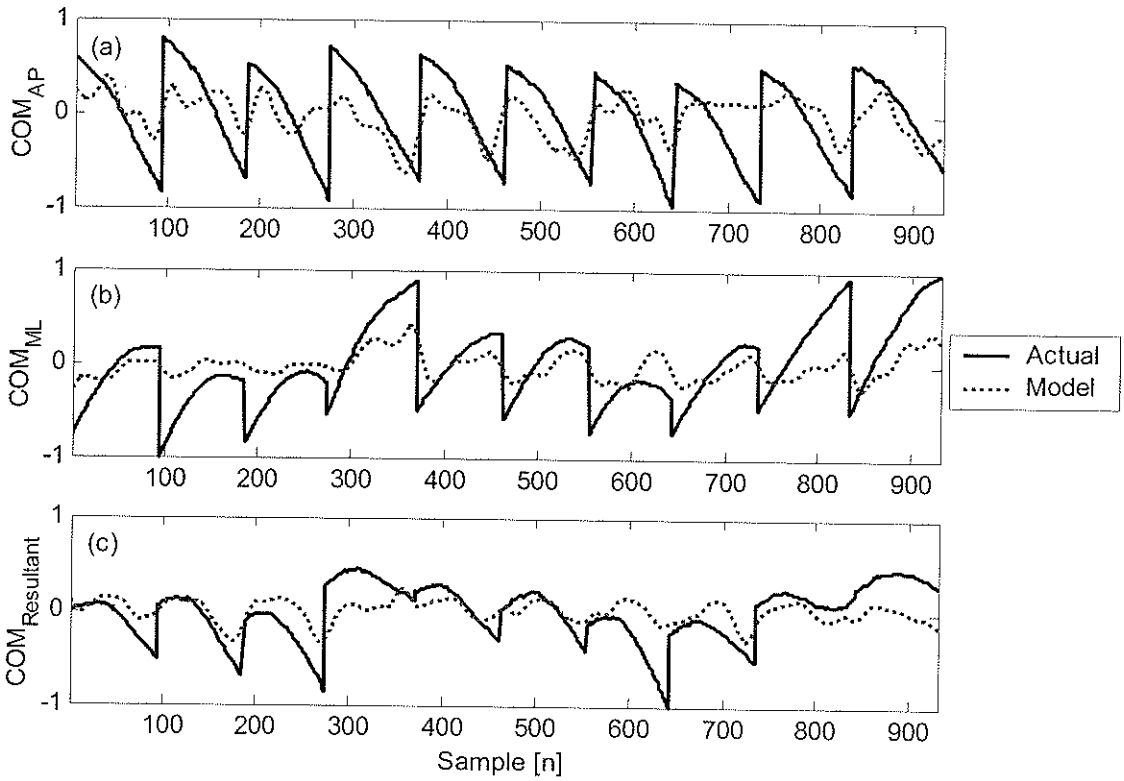

Figure 4.3 Adaptive fuzzy inference model results: normalized actual and developed COM trajectories in (a) A-P direction, (b) M-L direction, and (c) resultant for a typical subject for the stepping task on foam pad No. 2 at a slow speed. For display purposes, the end point of the previous forward step is connected to the start point of the next forward step.

Table 4.1 Adaptive Fuzzy Inference Model Error.

Task Condition (Surface, Speed)	A-P direction			M-L direction			Resultant		
	Mean ± SD Error (%)	Min Error (%)	Max Error (%)	Mean ± SD Error (%)	Min Error (%)	Max Error (%)	Mean ± SD Error (%)	Min Error (%)	Max Error (%)
Fixed, Normal	14.5±2.7	9.6	22.9	21.3±1.8	16.4	24.1	14.0±2.8	9.5	20.4
Fixed, Slow	13.6±3.6	7.9	21.4	21.8±2.6	15.7	27.0	10.7±2.3	6.7	14.9
Foam Pad 1, Normal	17.2±2.1	12.5	20.2	22.7±3.2	16.0	28.3	11.2±2.0	7.4	15.2
Foam Pad 2, Normal	15.5±2.0	11.3	20.8	21.6±2.6	16.8	27.2	11.6±2.3	7.3	19.9
Foam Pad 2, Slow	14.6±3.5	9.5	23.4	22.0±3.7	12.0	27.2	11.3±3.5	6.4	18.7

Based on the leave-one-out procedure, the model was tested using the left-out data, which was independent from the training data. This leads to testing the capability of the model to generalize differences in step duration or shifts in the signal baseline. The mean, standard deviation, minimum and maximum values of the adaptive fuzzy inference model error for each task condition in the A-P direction, M-L direction, and for the resultant are shown in Table 4.1.

4.1.2 Genetic Algorithm Sum-of-Sines Model

The genetic algorithm sum-of-sines model developed in [Betker *et al.*, 2006] was implemented to operate on single input. As swing leg and trunk accelerations are system inputs in this thesis, each input was separately applied to the model. The following sections describe two genetic algorithm sum-of-sines models for swing leg and trunk acceleration, respectively.

4.1.2.1 Swing Leg Acceleration

A genetic algorithm sum-of-sines model for swing leg acceleration was trained and tested for each of the seven stepping trials. The results for a typical subject for the task condition on a firm surface at a normal speed in the A-P direction, M-L direction, and for the resultant trajectory are shown in Figure 4.4. The results for a typical subject for the task condition on foam pad No. 2 at slow a speed in the A-P direction, M-L direction, and for the resultant trajectory are shown in Figure 4.5. Based on the leave-one-out procedure, the model was tested using the left-out data which was independent from the training data. This leads to testing the capability of the model to generalize differences in step duration or shifts in the signal baseline. The mean, standard deviation, minimum and maximum values of the genetic algorithm sum-of-sines model (for the swing leg)

error for each task condition in the A-P direction, M-L direction, and for the resultant trajectory are shown in Table 4.2.

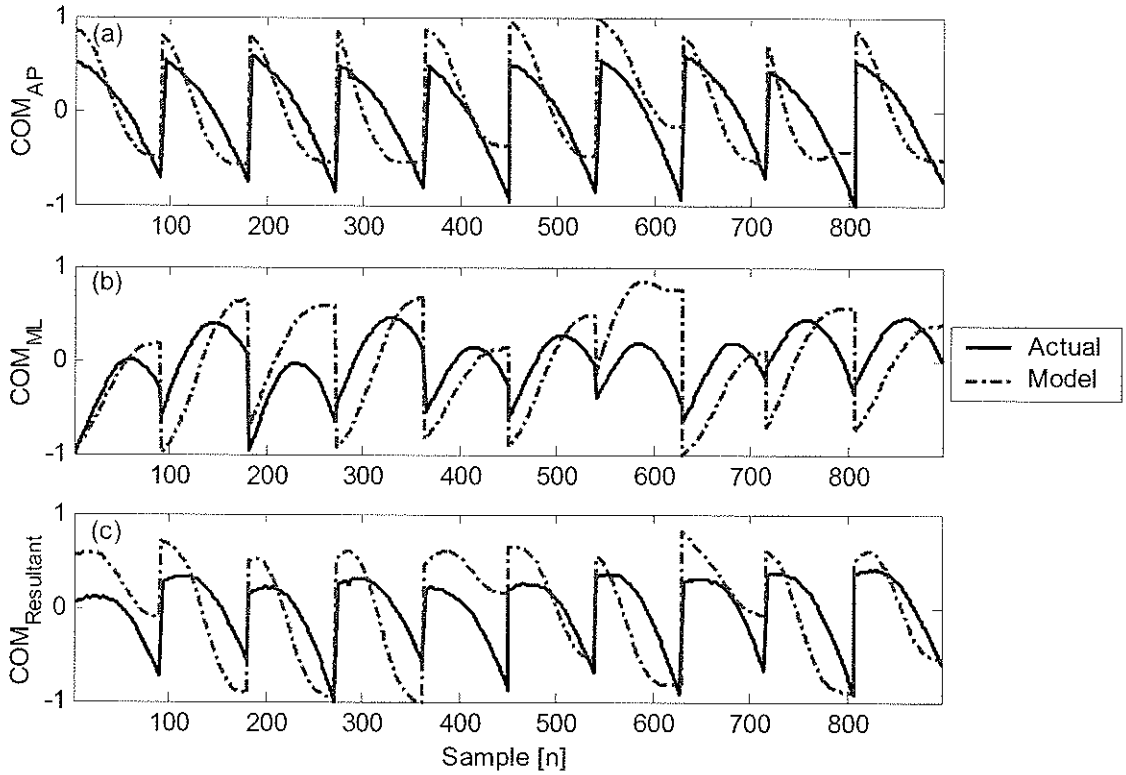

Figure 4.4 Genetic algorithm sum-of-sines model for the swing leg: normalized actual and developed COM trajectories in (a) A-P direction, (b) M-L direction, and (c) resultant for a typical subject for the stepping task on a fixed surface at a normal speed. For display purposes, the end point of the previous forward step is connected to the start point of the next forward step.

Table 4.2 Genetic Algorithm Sum-of-Sines Model (Swing Leg Acceleration).

Task Condition (Surface, Speed)	A-P direction			M-L direction			Resultant		
	Mean ± SD Error (%)	Min Error (%)	Max Error (%)	Mean ± SD Error (%)	Min Error (%)	Max Error (%)	Mean ± SD Error (%)	Min Error (%)	Max Error (%)
Fixed, Normal	19.5±5.5	11.5	29.7	22.0±5.8	11.5	35.4	20.5±5.8	12.9	37.0
Fixed, Slow	21.6±5.3	10.0	30.0	22.3±3.4	14.2	27.3	15.4±4.8	7.7	24.9
Foam Pad 1, Normal	24.2±7.2	12.8	38.4	21.5±6.6	11.7	35.5	17.3±3.7	11.7	23.8
Foam Pad 2, Normal	20.8±5.8	10.5	35.3	21.4±5.4	12.2	30.7	17.6±4.3	12.3	35.4
Foam Pad 2, Slow	22.4±6.4	12.0	36.3	23.2±6.3	12.2	35.8	17.4±4.8	6.5	25.3

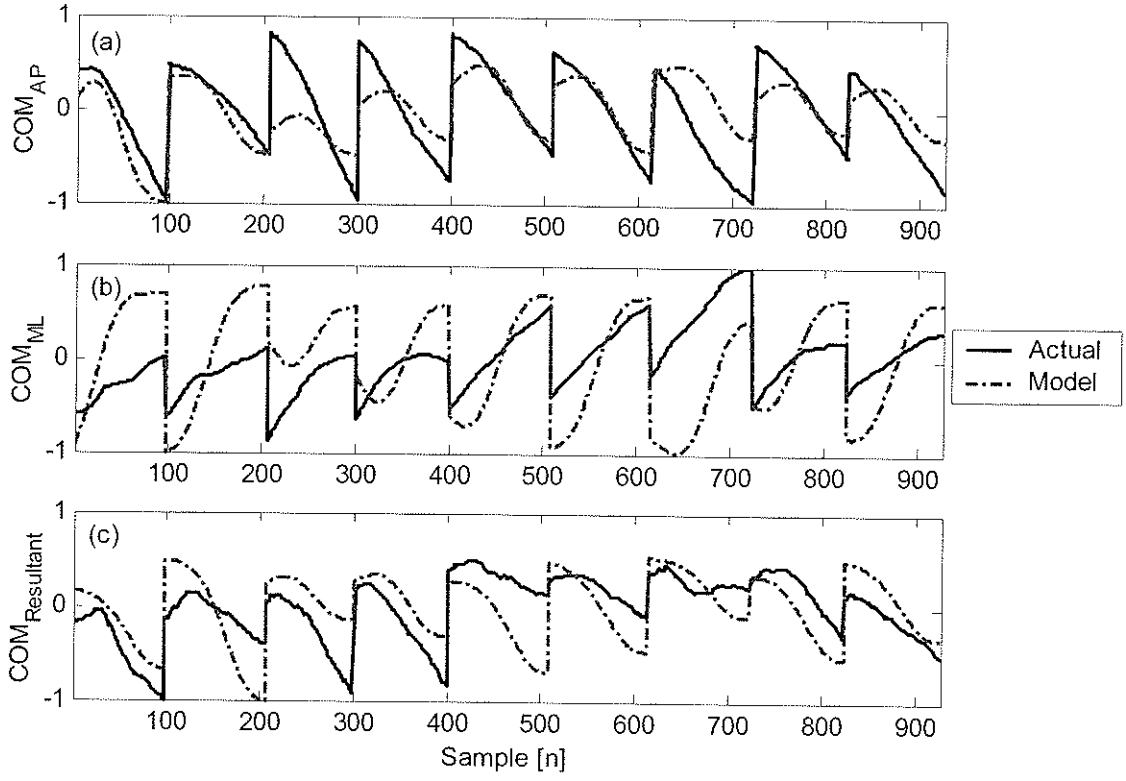

Figure 4.5 Genetic algorithm sum-of-sines model for the swing leg: normalized actual and developed COM trajectories in (a) A-P direction, (b) M-L direction, and (c) resultant for a typical subject for a stepping task on foam pad No. 2 at a slow speed. For display purposes, the end point of the previous forward step is connected to the start point of the next forward step.

4.1.2.2 TRUNK ACCELERATION

A genetic algorithm sum-of-sines model for the trunk acceleration was trained and tested for each of the seven stepping trials. The results for a typical subject for the task condition on a firm surface at a normal speed in the A-P direction, M-L direction, and for the resultant trajectory are shown in Figure 4.6. The results for a typical subject for the task condition on foam pad No. 2 at slow a speed in the A-P direction, M-L direction, and for the resultant trajectory are shown in Figure 4.7. Based on the leave-one-out procedure, the model was tested using the left-out data which was independent from the training data. This leads to testing the capability of the model to generalize differences in step duration or shifts in the signal baseline. The mean, standard deviation, minimum and maximum values of the genetic algorithm sum-of-sines model (for the trunk acceleration) error for each task condition in the A-P direction, M-L direction, and for the resultant trajectory are shown in Table 4.3.

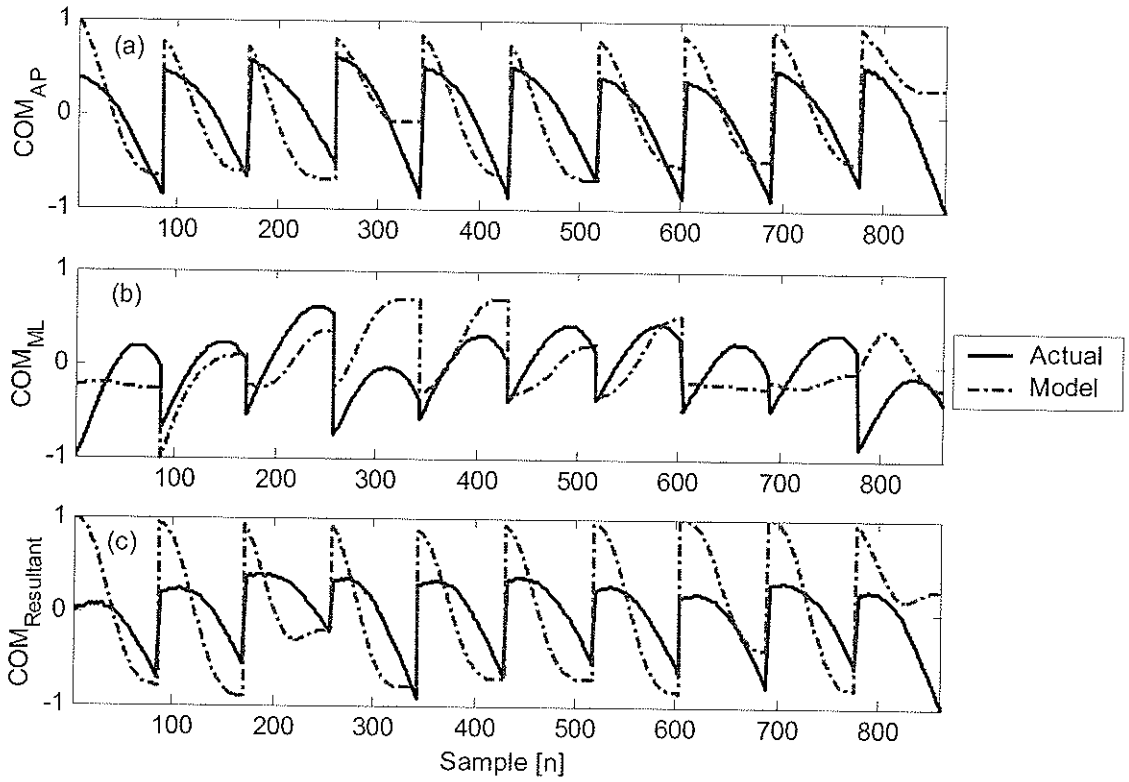

Figure 4.6 Genetic algorithm sum-of-sines model for the trunk: normalized actual and developed COM trajectories in (a) A-P direction, (b) M-L direction, and (c) resultant for a typical subject for the stepping task on a fixed surface at a normal speed. For display purposes, the end point of the previous forward step is connected to the start point of the next forward step.

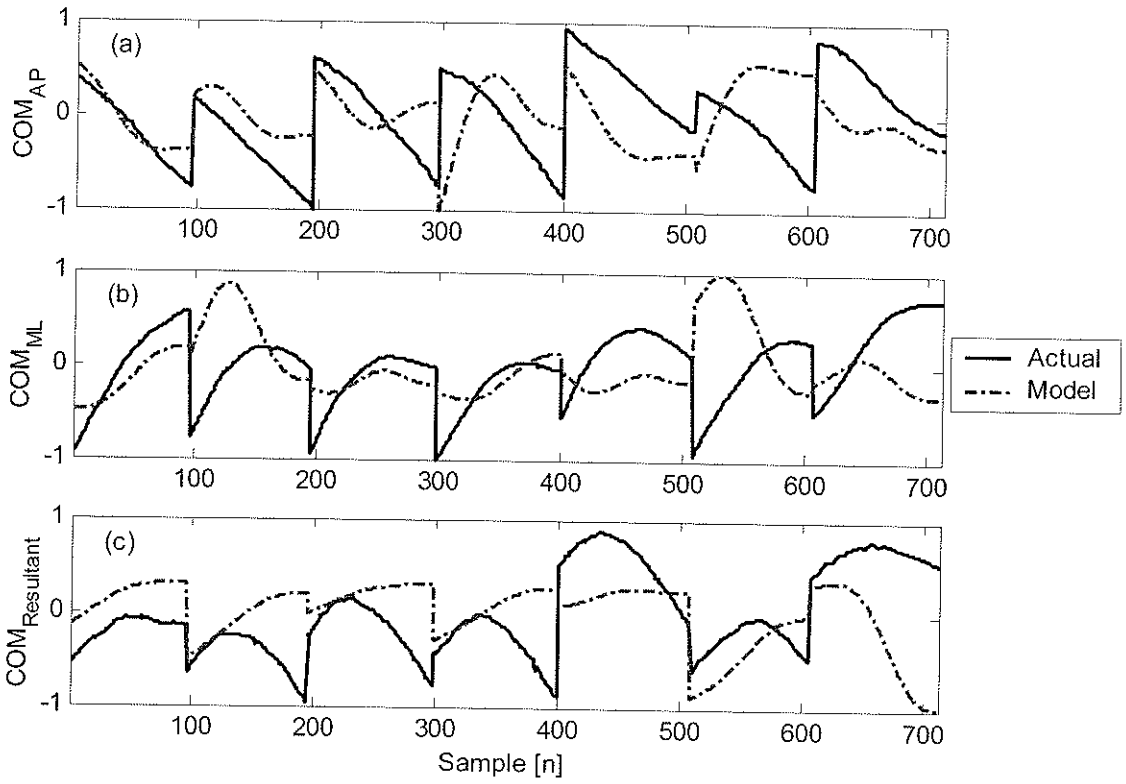

Figure 4.7 Genetic algorithm sum-of-sines model for the trunk: normalized actual and developed COM trajectories in (a) A-P direction, (b) M-L direction, and (c) resultant for a typical subject for the stepping task on foam pad No. 2 at a slow speed. For display purposes, the end point of the previous forward step is connected to the start point of the next forward step.

Table 4.3 Genetic Algorithm Sum-of-Sines Model (Trunk Acceleration).

Task Condition (Surface, Speed)	A-P direction			M-L direction			Resultant		
	Mean ± SD Error (%)	Min Error (%)	Max Error (%)	Mean ± SD Error (%)	Min Error (%)	Max Error (%)	Mean ± SD Error (%)	Min Error (%)	Max Error (%)
Fixed, Normal	13.4±2.7	8.7	19.8	19.7±3.7	13.8	28.5	20.3±3.8	14.6	31.2
Fixed, Slow	18.4±4.4	13.1	30.9	26.8±6.2	17.0	40.6	19.8±5.6	11.1	31.0
Foam Pad 1, Normal	20.8±2.8	12.4	24.0	17.8±4.0	10.1	24.2	17.0±3.4	11.7	23.8
Foam Pad 2, Normal	18.5±2.4	12.4	22.7	21.2±5.6	12.3	34.2	18.3±3.8	12.0	28.5
Foam Pad 2, Slow	18.6±5.3	10.4	34.3	23.5±5.7	12.2	35.8	16.9±4.2	10.6	23.2

4.1.3 GENETIC ALGORITHM PARABOLIC MODEL

Figure 4.8 depicts the parabolic relationship between the body accelerations (trunk and swing leg) and COM, in A-P direction, M-L direction, and for the resultant. Although the pattern of the parabolic relationship in the A-P direction is different from the one in the M-L direction, it is rather consistent in each given direction. A genetic algorithm was used to update the parameters that describe this parabolic relationship. The following paragraphs describe the results for the model.

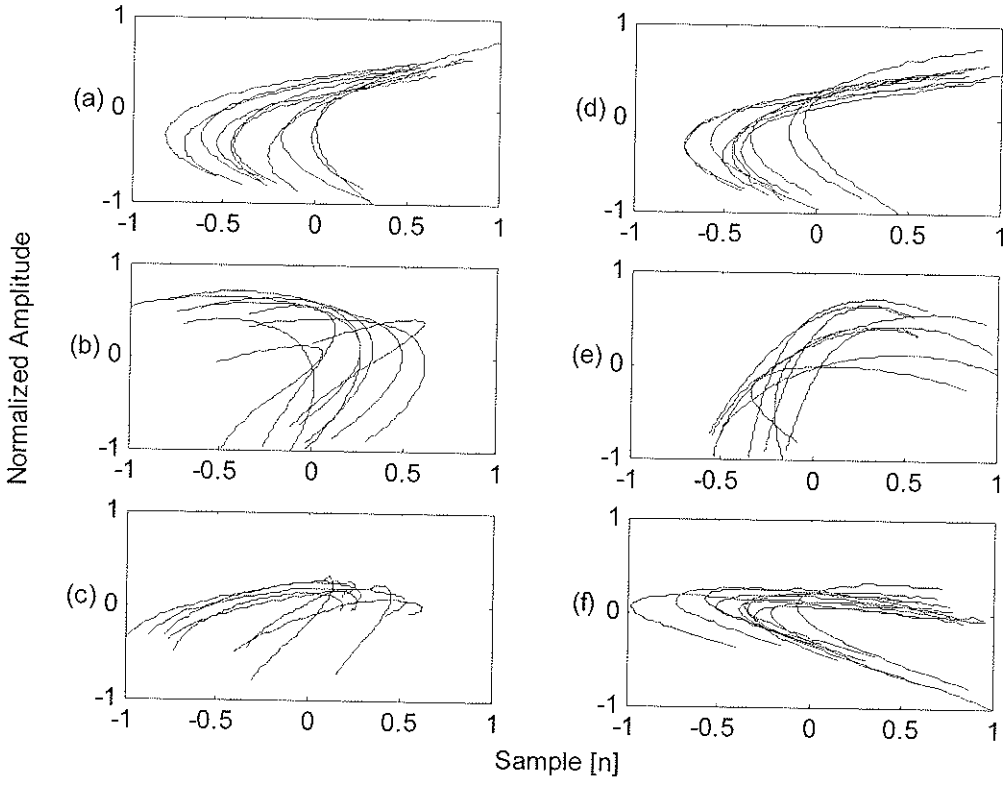

Figure 4.8 The parabolic relationship between the COM and swing leg acceleration for a typical subject in (a) the A-P direction, (b) the M-L direction, and (c) for the resultant, and between the COM and trunk acceleration for a typical subject in (d) the A-P direction, (e) the M-L direction, and (f) for the resultant.

A genetic algorithm parabolic model for the trunk and swing leg accelerations was trained and tested for each of the seven stepping trials. The results for a typical subject for the task condition on a firm surface at a normal speed in the A-P direction, M-L direction, and for the resultant trajectory are shown in Figure 4.9. The results for a typical subject for the task condition on foam pad No. 2 at a slow speed in the A-P direction, M-L direction, and for the resultant trajectory are shown in Figure 4.10. Based on the leave-one-out procedure, the model was tested using the left-out data which was independent from the training data. This leads to testing the capability of the model to generalize differences in step duration or shifts in the signal baseline. The mean, standard deviation, minimum and maximum values of the COM model error for each task condition in the A-P direction, M-L direction, and for a combination of the two directions are shown in Table 4.4.

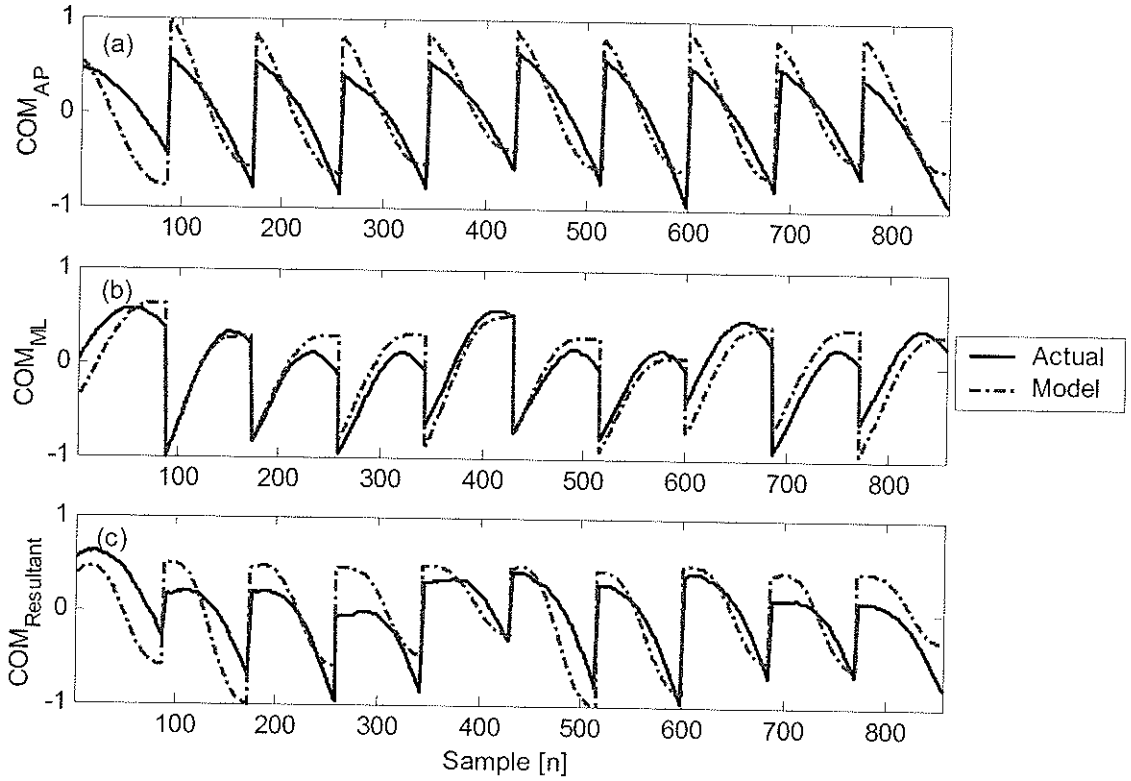

Figure 4.9 Genetic algorithm parabolic model: normalized actual and developed COM trajectories in (a) A-P direction, (b) M-L direction, and (c) resultant for a typical subject for the stepping task on a fixed surface at a normal speed. For display purposes, the end point of the previous forward step is connected to the start point of the next forward step.

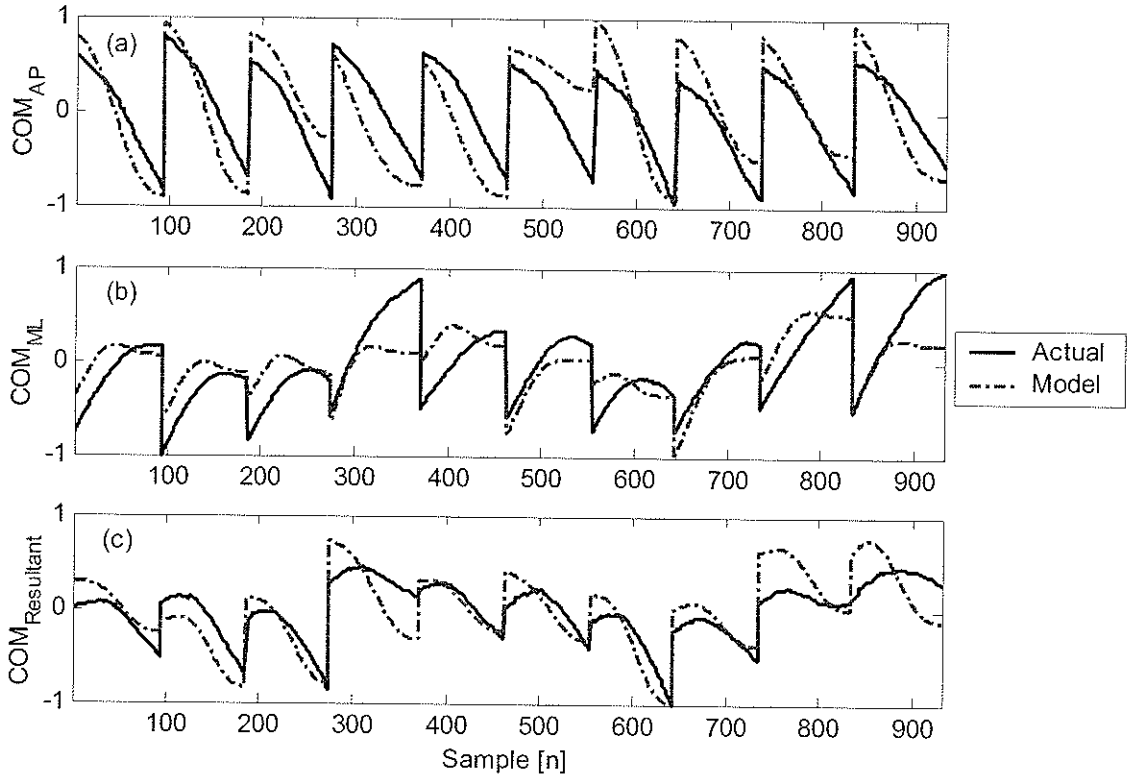

Figure 4.10 Genetic algorithm parabolic model: normalized actual and developed COM trajectories in (a) A-P direction, (b) M-L direction, and (c) resultant for a typical subject for the stepping task on foam pad No. 2 at a slow speed. For display purposes, the end point of the previous forward step is connected to the start point of the next forward step.

Table 4.4 Genetic Algorithm Parabolic Model.

Task Condition (Surface, Speed)	A-P direction			M-L direction			Resultant		
	Mean ± SD Error (%)	Min Error (%)	Max Error (%)	Mean ± SD Error (%)	Min Error (%)	Max Error (%)	Mean ± SD Error (%)	Min Error (%)	Max Error (%)
Fixed, Normal	5.7 ±2.5	3.1	14.2	17.4±5.0	9.8	29.4	9.7±2.2	5.9	15.5
Fixed, Slow	8.0±2.9	4.1	13.6	12.3±3.2	5.7	17.0	12.9±4.7	6.3	22.2
Foam Pad 1, Normal	8.9±3.3	5.4	17.0	15.5±4.8	9.9	25.7	17.2±4.5	9.3	26.5
Foam Pad 2, Normal	9.5±2.0	4.8	13.5	15.4±3.4	8.7	21.3	10.8±4.0	5.8	23.0
Foam Pad 2, Slow	12.9±2.8	8.3	16.5	17.6±5.2	11.3	25.7	14.1±4.4	6.9	25.3

4.2 TRUNK ACCELERATION VARIABILITY

Trunk acceleration variability was computed in both the A-P and M-L directions for each task condition (Table 4.5). A statistically significant difference ($p<0.05$) in trunk acceleration variability between the A-P and M-L directions was only found during the first task condition; forward stepping on fixed surface at normal speed.

Table 4.5 Trunk Acceleration Variability.

Task Condition (Surface, Speed)	A-P direction			M-L direction		
	Mean±SD	Min	Max	Mean±SD	Min	Max
Fixed, Normal*	0.31±0.20	<0.01	0.67	0.66±0.18	0.15	0.94
Fixed, Slow	0.27±0.20	<0.01	0.68	0.26±0.20	<0.01	0.71
Foam pad 1, Normal	0.38±0.13	0.13	0.59	0.37±0.17	0.04	0.64
Foam pad 2, Normal	0.36±0.16	<0.01	0.68	0.29±0.18	0.03	0.69
Foam pad 2, Slow	0.15±0.12	<0.01	0.42	0.15±0.13	<0.01	0.47

Note: The task condition with a significantly higher variability in the M-L direction than that in the A-P direction is marked with an asterisk (*).

4.3 CHARACTERISTICS OF THE COP

4.3.1 RÉNYI DIMENSION AND SPECTRUM

The averaged Rényi spectrum computed from the COP trajectories during forward stepping at a moment order of q ranging from 0 to 9 is shown in Figure 4.11. The Rényi dimension at any moment order of q can be obtained from the Rényi spectrum. The Rényi dimensions for each task condition were between 1 and 2; this is as expected since the Euclidean dimension D_E of the COP trajectory is larger than that of a line object ($D_E = 1$), but smaller than that of a surface object ($D_E = 2$).

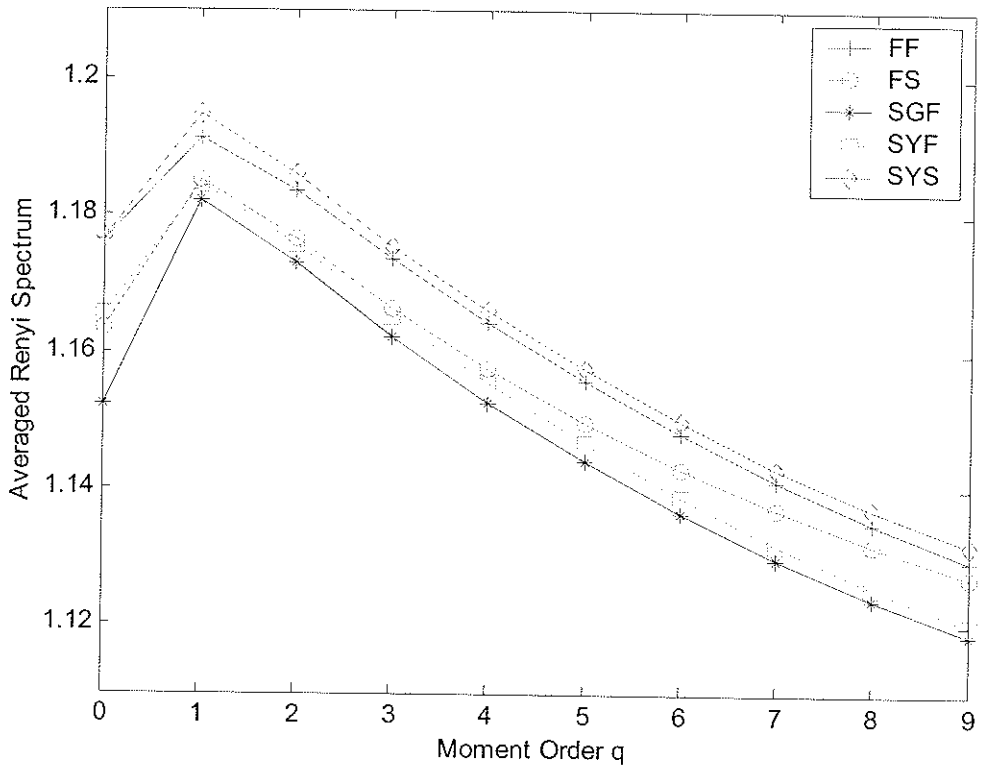

Figure 4.11 The averaged Rényi spectrum of the COP trajectories during forward stepping is shown for: FF, the task on the firm normal fixed surface at a normal speed; FS, the task on the firm normal fixed surface at a slow speed; SGF, the task on foam pad No. 1 at a normal speed; SYF, the task on foam pad No. 2 at a normal speed; and SYS, the task on foam pad No. 2 at a slow speed.

Figure 4.12 depicts the averaged Rényi dimension at a moment order q of 2, which is the correlation dimension D_C. The mean, standard deviation, minimum and maximum values of the Rényi dimension D_2 for each task condition are presented in Table 4.6.

Table 4.6 Averaged Rényi Dimension at Moment Order q of 2.

Task condition (Surface, Speed)	Mean ± SD	Minimum	Maximum
Fixed, Normal	1.1835 ± 0.0448	1.0807	1.2176
Fixed, Slow	1.1764 ± 0.0475	1.0699	1.2594
Foam pad 1, Normal	1.1729 ± 0.0405	1.0592	1.2024
Foam pad 2, Normal	1.1724 ± 0.0399	1.0691	1.2157
Foam pad 2, Slow	1.1857 ± 0.0572	1.0340	1.2315

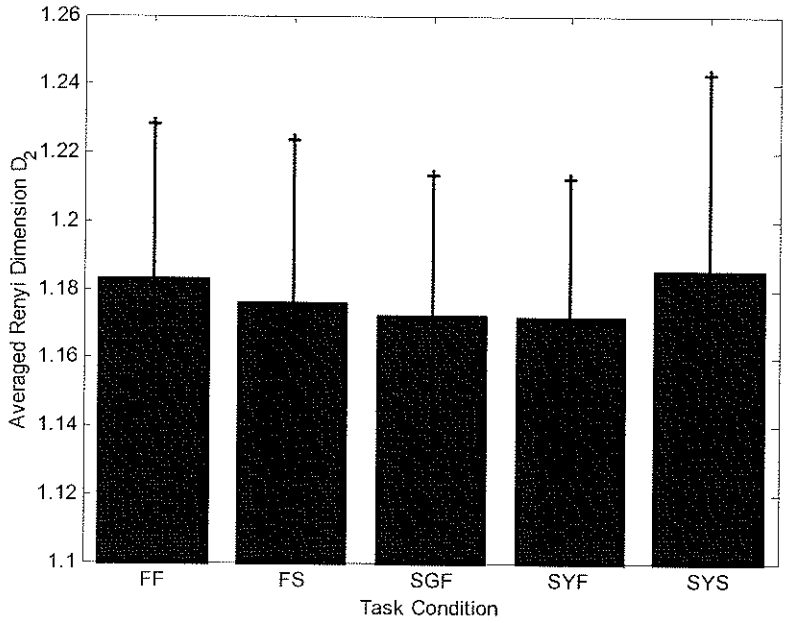

Figure 4.12 The averaged Rényi dimension D_2 for each task condition (mean ± standard deviation) is shown for: FF, the task on the firm normal fixed surface at a normal speed; FS, the task on the firm normal fixed surface at a slow speed; SGF, the task on foam pad No. 1 at a normal speed; SYF, the task on foam pad No. 2 at a normal speed; and SYS, the task on foam pad No. 2 at a slow speed.

4.3.2 Sway Path Length

The averaged sway path length computed from the COP trajectories during forward stepping for each task condition are shown in Figure 4.13. The sway path length was decreased when the surface and/or speed condition was altered. The effect of surface condition on sway path length was less evident than that of the speed condition. The mean, standard deviation, minimum and maximum values of the sway path length for each task condition are presented in Table 4.7.

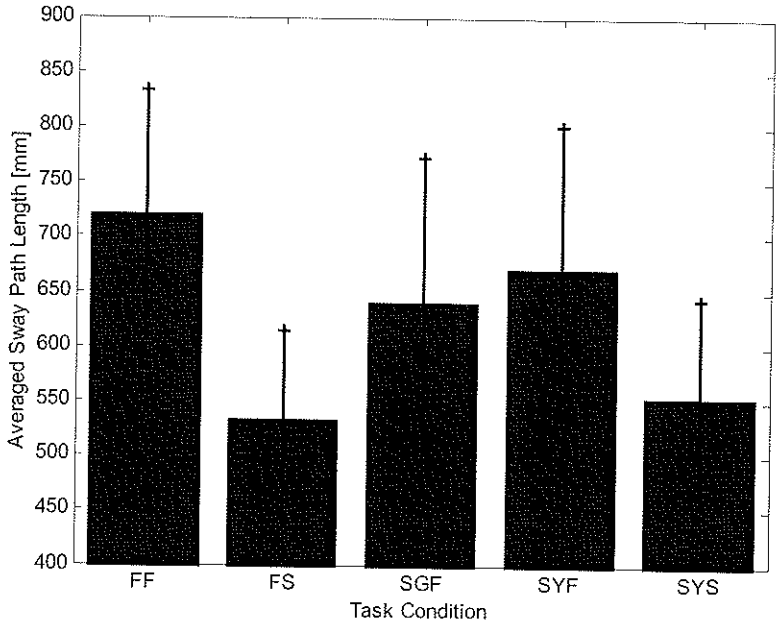

Figure 4.13 The averaged sway path length for each task condition (mean ± standard deviation) is shown for: FF, the task on the firm normal fixed surface at a normal speed; FS, the task on the firm normal fixed surface at a slow speed; SGF, the task on foam pad No. 1 at a normal speed; SYF, the task on foam pad No. 2 at a normal speed; and SYS, the task on foam pad No. 2 at a slow speed.

Table 4.7 Averaged Sway Path Length of the COP Trajectory.

Task Condition (Surface, Speed)	Resultant		
	Mean ± SD [mm]	Minimum [mm]	Maximum [mm]
Fixed, Normal	721.5 ± 112.1	486.3	923.1
Fixed, Slow	533.2 ± 81.3	445.5	721.0
Foam Pad 1, Normal	639.8 ± 133.0	446.4	844.6
Foam Pad 2, Normal	671.8 ± 129.4	425.5	891.1
Foam Pad 2, Slow	554.7 ± 88.5	440.3	787.0

CHAPTER 5

DISCUSSION

The main findings of this thesis are as follows. As expected, the two task conditions, support surface and stepping speed, provided ample environmental uncertainty to the system. Three models were generated, among which the genetic algorithm parabolic model showed the best performance for modeling the COM trajectories using the trunk and swing leg accelerations. COM modeling error in the M-L direction was higher than that in the A-P direction. An increase in trunk acceleration variability was found in one task only, namely stepping on a fixed surface at a normal stepping speed. Trunk acceleration variability in the M-L direction was significantly higher than that in the A-P direction, when the subjects performed stepping on a fixed surface at a normal speed. Between the tasks, there was no significant difference in the Rényi dimension of the COP trajectories. However, a significant difference was found in the sway path length of the COP trajectories between normal and slow speed stepping.

5.1 COM IN RELATION TO ACCELERATION

In order to examine the relationship between the COM trajectories and body accelerations, video-based motion measurement system and accelerometers were utilized in this thesis. The present results showed that body accelerations can be used to estimate the COM trajectories. The use of accelerometer showed potential as it is portable and much less expensive than fixed force plate and/or video-based motion measurement system. Thus an accelerometer system is available for daily clinical practice,

independent of location or setting. However, various biomechanical models, e.g. models developed in [Chan, 1999; Lapond *et al.*, 2004, Barbier *et al.*, 2006], used fixed force plate and/or video-based motion measurement system to estimate the COM trajectories. As these systems are not portable but fixed, they are not available for a routine clinical assessment. Therefore, the use of body accelerations on estimating the COM trajectories has been a motivating research subject. In fact, many researchers [Morris, 1973; Kane *et al.*, 1974; Light *et al.*, 1980; Gilbert *et al.*, 1984] used the body segmental acceleration to study the body segmental kinematics. [Wu and Ladin, 1996] showed that the linear acceleration and angular velocity measurements play a dominant role in increasing the frequency range of the estimated COM; they concluded that the body segmental accelerations can increase the accuracy of COM estimation. Recent studies [Mayagoitia *et al.*, 2002; Moe-Nilssen and Helbostad, 2004; Luinge and Veltink, 2005; Lyons *et al.*, 2005; Karantonis *et al.*, 2006] also used accelerometers to examine kinematics during walking; their results demonstrated that data obtained from miniature inexpensive accelerometers can approximate human kinematics during walking as accurately as a video motion analysis system. In a recent study, [Betker *et al.*, 2006] showed that during quiet stance the COM trajectory could be approximated using body acceleration; this is a promising result, indicating that the kinematics of human stepping tasks may also be estimated using an accelerometer system. Although it showed potential, the accelerometer system in this thesis depended on a kinematic parameter from video-based motion measurement system, i.e. the vertical position of the ankle marker placed on swing leg. This kinematic parameter was necessary to detect and extract the forward stepping phase from swing foot lift to heel strike. In order to truly estimate the COM

trajectories using body accelerations, a further study is required to be independent of video-based motion measurement system.

During the single stepping task, two conditions were utilized in this thesis: support surface and stepping speed. The compliant surface introduced an environmental challenge into the system. A slower step speed was used to increase the duration of the single support stance. Both of these conditions would increase task difficulty. The present results show that the error in all models increased when a compliant surface was used and when the step speed was slow. This was expected as CNS interpretation of somatosensory information was distorted by the compliant surface and the increased duration of the single support stance during slow stepping increased the balance requirements. The use of the compliant surface on balancing task was investigated by [Teasdale *et al.*, 1991]; they have shown that standing and balancing on a compliant surface is a difficult task for even healthy individuals with no history of balance problems. [Lajoie *et al.*, 1993] have suggested that reaction times when subjects were in single support phase were significantly longer than those in double support phase; the attentional (cognitive) demands increased with an increase in the balance requirements of the single support stance. Therefore both of task conditions utilized in this thesis, i.e. the compliant surface and slower step speed, provided environmental uncertainty to the balance system.

Among the three developed models in this thesis, the genetic algorithm parabolic model showed the best performance describing the COM trajectory's relationship with the trunk and swing leg acceleration. The genetic algorithm sum-of-sines model performed well during quiet stance in [Betker *et al.*, 2006], but the present results showed

that it did not performed well during forward stepping. This was expected as the pattern of parabolic relationship between COM trajectories and body accelerations (depicted in Figure 4.8) was observed. The mean error of the genetic algorithm parabolic model was within 14.1%, while that of the genetic algorithm sum-of-sines model was within 20.5% (trunk acceleration) and 20.3% (swing leg acceleration). The present results showed that the model errors in the M-L direction were significantly greater than those in the A-P direction; that might be a result of the increase in the M-L magnitude range of the body segment motions, such as the swing foot. In order to prevail over the balance disturbance and maintain stability, the swing foot trajectory should be modified to set the foot down at a position that would establish a new base of support. In [Chou *et al.*, 2003], a positive correlation between increased COM motion in the M-L direction and the magnitude of the swing foot trajectory in the M-L direction was observed. The finding of the increased COM motion in the M-L direction is also addressed in [Greenspan *et al.*, 1998], where the importance of fall characteristics during walking were studied. They found that compared to healthy elderly subjects, the elderly exhibiting symptoms of dizziness or unsteadiness showed a significantly greater and faster motion of the COM in the M-L direction.

5.2 Trunk Acceleration Variability

Subjects were forced to use feedback controls and not feedforward predictions. Balance task is implemented to examine how balance control system reacts to unexpected disturbance or unsuccessful feedforward control. In order to challenge their balance strategies in feedback control scheme, they were instructed not to look down during forward stepping; otherwise visual information will help the CNS predict disturbances

based on prior experience or memory. The use of feedback controls produces more movement errors, which may cause increased variability in body segment motions, such as trunk accelerations, and also increased COP excursions resulting in an increased COP path length. However, according to the present findings, those increases did not happen for all stepping tasks; a significant increase in trunk acceleration variability was found in one task only: stepping on fixed surface and at normal stepping speed. The COP path length during stepping on a fixed surface at a normal speed was longer than that on the foam pad at a slow speed. Due to the practice steps performed prior to each stepping task, subjects knew the surface was altered to a less stable one. Hence, they consciously became more cautious; this could have lead to less kinematic variability in the trunk accelerations and a shorter COP path length.

This cautious behaviour was examined in [Menz *et al.*, 2003a, Menz *et al.*, 2003b, Menz *et al.*, 2003c], where subjects were asked to walk on a normal fixed surface and then on a compliant/irregular surface. Their results showed that subjects' speed and step length were decreased when walking on the compliant surface, as compared to walking on the normal surface. This suggests that when walking on a compliant surface, subjects perceived a threat to their stability and subsequently employed a more conservative pattern in attempt to minimize body movement. The destabilizing effect experienced with a compliant/irregular surface on cautious behaviour was discussed in [MacLellan and Patla, 2006], where movement strategy during self-paced walking on a visible compliant surface was studied. They suggested that a person who previously experienced a threatening environment would become more cautious when walking on a compliant/irregular surface. Experience could assist the CNS to better predict the

potential threat of the compliant/irregular surface and cause a more cautious stepping pattern. In this case, the visual system plays a role in providing the characteristics of the compliant surface prior to feedforward controls. This is similar to the present study where the surface change was obviously visible and a few practice steps on altered surface were performed.

In [Barak *et al.*, 2006], the elderly fallers showed increased kinematic variability during walking when compared with non-fallers. It was concluded that increased variability may be an important gait risk factor in the elderly with a history of falls. [Moe-Nilssen and Helbostad, 2005] studied this increased variability particularly in trunk accelerations, since the size and mass of the trunk segment are much greater than those of the pelvis and legs; thus, trunk motion contributes to total body COM motion more than any other body segment [Grabiner *et al.*, 1993]. According to [Moe-Nilssen and Helbostad, 2005], the stride-to-stride variability in the M-L trunk acceleration may represent a different aspect of motor control and it may provide the ability to discriminate impaired balance control. The present findings, listed in Table 4.5, showed that trunk acceleration variability in the M-L direction was significantly higher than that in the A-P direction ($p<0.05$); this is consistent with the findings of [Moe-Nilssen and Helbostad, 2005]. However it was valid for only one task, namely stepping on a fixed surface at a normal speed. This may suggest that the subjects became more cautious when they performed more challenging task conditions and thus, there was less variability in body motion during those tasks.

The results in Table 4.5 also showed that the lowest trunk acceleration variability was observed during the most difficult task (stepping on foam pad No. 2 at a slow speed).

However, balance control on a compliant surface is intuitively more difficult than on a normal fixed surface. Thus, there is more variability in the body segment motions, which may cause a higher modeling error. The results of the developed models (Tables 4.1 to 4.4) indicate that model errors in both the A-P and M-L directions increase with compliant surfaces and the slow speed condition. This may indicate that trunk acceleration variability has no effect on modeling error.

5.3 Fractal Analysis of the COP

The Rényi dimension of the COP trajectory during forward stepping did not increase with task difficulty, except for the task on foam pad No. 2 at a slow speed; in this case, the Rényi dimension slightly increased. Also, there was no statistically significant difference in the Rényi dimension between task conditions. Similar results were found in [Han *et al.*, 2004], where the Rényi dimension of the control group remained constant, except for a slight increase in the Rényi dimension for the most demanding task, where somatosensory information was distorted by a foam pad surface and vision was eliminated. An increase in the fractal dimension may indicate the use of less stable control strategies or a higher tendency for instability [Doyle *et al*, 2004; Błaszczyk and Klonowski, 2001]. However, no significant increase in the fractal dimension may imply that subjects participated in this thesis used stable control strategies, which agrees with the subjects' history free from neurological disorder or postural difficulties. For comparison purpose, the Rényi dimension of patients during forward stepping would further support the present results; it will strengthen the Rényi dimension's feasibility in detecting balance instability. The recruitment of patients group in a future study is then recommended.

In addition to the Rényi dimension, the linear measure, the sway path length, was used to investigate any significant difference from the nonlinear measure, the Rényi dimension. The present results showed that the sway path length did change with task difficulty; the sway path length during forward stepping at normal speed was longer than that at slow speed. This pattern may be affected by cautious behaviour that was discussed in the previous section. When subjects perceived a threat to their balance stability, they subsequently employed a more conservative pattern in attempt to minimize body movement. The effect of cautious behaviour on the sway path length is greater than that of the compliant surface. This may indicate that balance strategies are more affected by cognitive system than environmental uncertainty. The pattern of the sway path length in the present study was different from the one observed in [Han *et al.*, 2004] where the sway path length during quiet stance increased as the task difficulty increased. This was expected as cautious behaviour is intuitively not the case in balance strategies during quiet stance; as a response to disturbance during standing still, ankle, hip or stepping strategy can be applied to maintain balance, depending on the degree of disturbance.

CHAPTER 6

CONCLUSION AND FUTURE WORK

6.1 CONCLUSION

This thesis aimed to develop a model of the COM trajectory during forward stepping as a function of trunk and swing leg accelerations. It was shown that the genetic algorithm parabolic model was able to estimate the COM trajectory within a mean error of 12.9% in the A-P direction, 17.6% in the M-L direction, and 17.2% for the resultant trajectory. The results are encouraging and pave the way for integrating the COM models with a balance assessment system.

Furthermore, motor variability was measured to examine whether the variability may indicate adaptability of human balance control. It was shown that the cautious behaviour of subjects could have guided to less trunk acceleration variability and thus shorter sway path length of the COP trajectories. Experience or knowledge could assist the CNS to better predict the potential balance risk.

In addition, the linear and nonlinear measures of the COP trajectories were compared to observe balance control behaviour of young healthy subjects. A significant difference was found in the linear measure, the sway path length of the COP trajectories between normal and slow speed stepping. The Rényi dimension, the nonlinear measure, did not show any significant difference between tasks. However, given that all subjects were young and healthy with no history of balance disorder, it is not conclusive to rule out the Rényi dimension's feasibility in detecting balance instability.

6.2 FUTURE WORK

Based on the developed model demonstrating the relationship between the COM trajectory and body acceleration, the COM trajectory could be well explained by body accelerations. However, the ankle position in the vertical direction was required to extract the forward steps and this kinematic information was obtained via a video-based motion analysis system. Having used a kinematic parameter from motion capture system to extract forward stepping phase, it is not reasonable to claim the developed model is able to independently estimate the COM trajectory using body accelerations; it is rather an investigation of relationship between the COM trajectory and body accelerations. Therefore study on the actual estimation of the COM trajectory using body accelerations, without the use of kinematic parameter from motion capture system, is strongly recommended as a future work.

Study on trunk acceleration variability revealed that subjects become more cautious and tend to employ more conservative balance pattern when they encounter with a balance threat. As all subjects participated in this thesis were young and healthy, the effect of environmental uncertainty on the elderly and people with postural balance problems is useful to further assist the present results. Investigating how patients or the elderly react to a balance threat is recommended as a future work.

The present results showed that the COM model error in the M-L direction was higher than that in the A-P direction. White noise from the data acquisition system may affect higher COM model error in the M-L direction. However the CNS is believed to be a dominant factor in higher error in the M-L direction; when the CNS received distorted and/or delayed information from sensory systems, the postural control and balance

strategy determined by the CNS would not succeed in all situations. Due to this observation, further study on identifying and understanding a dominant source of higher error in M-L direction during forward stepping is recommended as future work.

No significant increase in the Rényi dimension of the COP trajectories between stepping tasks was found. However one can not exclude the Rényi dimension as the indicator of instable balance strategies as all subjects in this thesis were young and healthy. In order to further support that the Rényi dimension represents a significant characteristic feature of instability, study on the Rényi dimension of patients or the elderly during forward stepping is recommended as a future work. The sway path length of patients during forward stepping is also recommended as a future work.

APPENDIX A

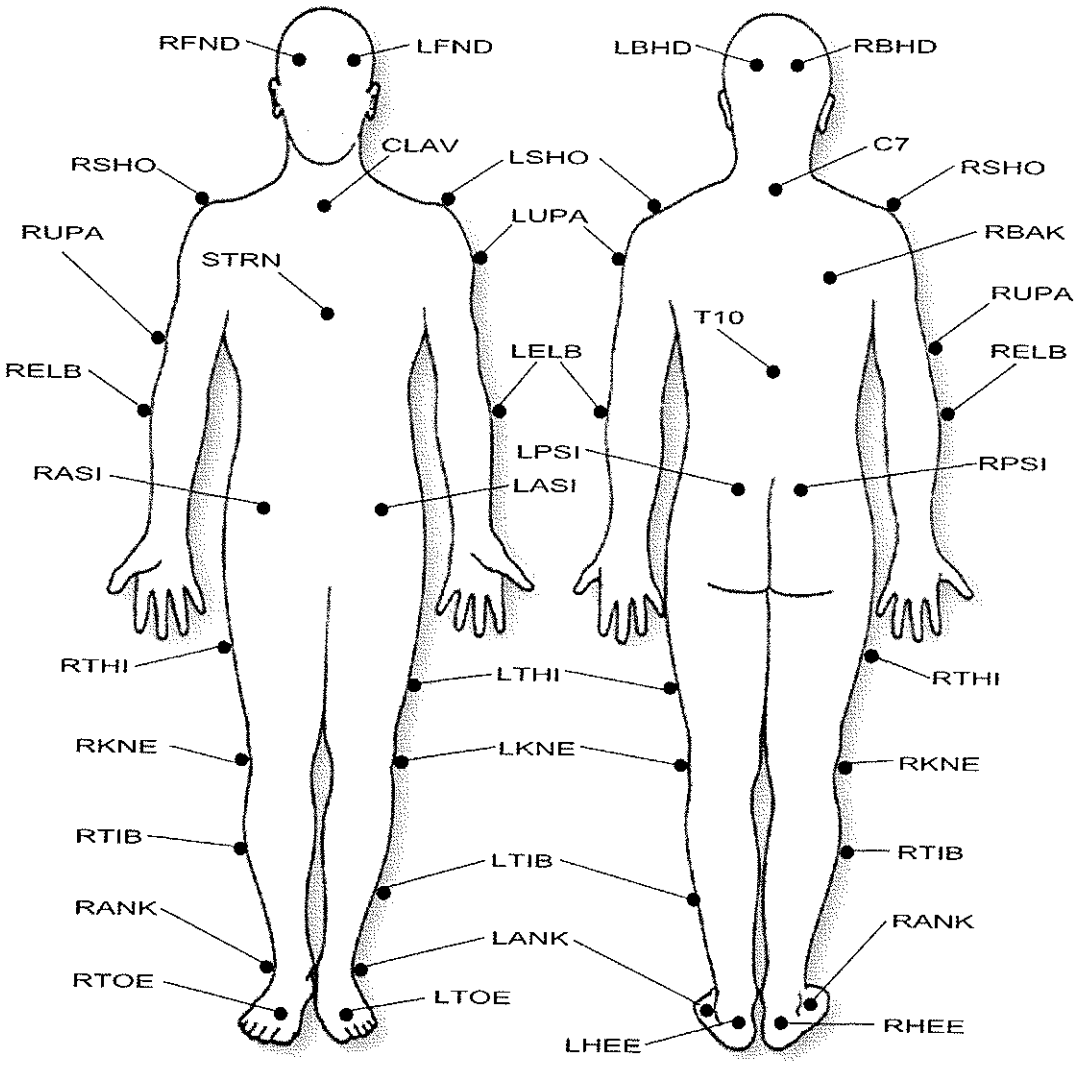

Figure A.1 PLUG-IN-GAIT MARKER PLACEMENT

A.1 UPPER BODY

A.1.1 HEAD MARKERS

LFHD	Left front head (left temple)
RFHD	Right front head (right temple)
LBHD	Left back head (in a horizontal plane of the front head markers)
RBHD	Right back head

A.1.2 TORSO MARKERS

C7	7th Cervical Vertebrae
T10	10th Thoracic Vertebrae
CLAV	Clavicle
STRN	Sternum
RBAK	Right back (the middle of the right scapula)

A.1.3 ARM MARKERS

LSHO	Left shoulder (the Acromio-clavicular joint)
RSHO	Right shoulder
LUPA	Left upper arm (between the elbow and shoulder markers)
RUPA	Right upper arm
LELB	Left elbow (lateral epicondyle approximating elbow joint axis)
RELB	Right elbow

A.2 LOWER BODY

A.2.1 PELVIS

LASI	Left ASIS (Anterior Superior Iliac Spine)
RASI	Right ASIS (Anterior Superior Iliac Spine)
LPSI	Left PSIS (Posterior Superior Iliac Spine)
RPSI	Right PSIS (Posterior Superior Iliac Spine)

A.2.2 LEG MARKERS

LKNE	Left knee (the lateral epicondyle)
RKNE	Right knee
LTHI	Left thigh (the lower lateral 1/3 surface of the thigh)
RTHI	Right thigh

LANK	Left ankle (the lateral malleolus along an imaginary line that passes through the transmalleolar axis)
RANK	Right ankle
LTIB	Left tibial wand (the lower 1/3 of the shank to determine the alignment of the ankle flexion axis)
RTIB	Right tibial wand

A.2.3 FOOT MARKERS

LTOE	Left toe (the second metatarsal head, on the mid-foot side of the equinus break between fore-foot and mid-foot)
RTOE	Right toe
LHEE	Left heel (the calcaneous at the same height above the plantar surface of the foot as the toe marker)
RHEE	Right heel

APPENDIX B

Specifications of Biometrics S2-10G-MF accelerometer

Output	0 to ±10G (0 to ±98.1 m/s2), 3 channels labelled X, Y, Z
Mass	10 g
Dimensions	19.0×12.7×10.9 mm (Length×Depth×Height)
Case Material	Anodised aluminium
Cable	Highly flexible grade, length 1800 mm
Supply Voltage	3.50 ~ 5.00 Vdc
Sensitivity	±100mV/G
Cross Talk	<5%
Accuracy	Better than ± 2% full scale
Bandwidth	DC to 100 Hz
Filter	8 pole, 8th order 1.2 Elliptic
Plugs	Direct connection to either DataLINK or DataLOG 3×Lemo 0B series 4 pin plugs corresponding to channels X, Y, Z
Shock Survival	500 G
Resolution	0.0025 G

REFERENCES

J. H. J. Allum and F. Honegger, "Interactions between vestibular and proprioceptive inputs triggering and modulating human balance-correcting responses differ across muscles", *Exp. Brain Res.*, vol. 121(4), pp. 478–94, 1998.

B. Auvinet, D. Chaleil and E. Barrey, "Accelerometric gait analysis for use in hospital outpatients", *Revue du Rhumatisme*, vol. 66(7–9), pp. 389–97, 1999.

Y. Barak, R. C. Wagenaar and K. G. Holt, "Gait characteristics of elderly people with a history of falls: a dynamic approach", *Phys. Ther.*, vol. 86(11), pp. 1501–10, 2006.

F. Barbier, P. Allard, K. Guelton, B. Colobert and A. P. Godillon-Maquinghen, "Estimation of the 3-D center of mass excursion from force-plate data during standing", *IEEE Trans. Neural Syst. Rehabil. Eng.*, vol. 11(1), pp. 31–7, 2003.

A. L. Betker, T. Szturm and Z. Moussavi, "Application of Feedforward Backpropagation Neural Network to Center of Mass Estimation for Use in a Clinical Environment", *IEEE Trans. Biol. Med.*, vol. 53(4), pp. 686–93, 2006.

J. W. Błaszczyk and W. Klonowski, "Postural stability and fractal dynamics", *Acta. Neurobiol. Exp.*, vol. 61(2), pp. 105–12, 2001.

E. J. Bradshaw and W. A. Sparrow, "Effects of approach velocity and foot-target characteristics on the visual regulation of step length", *Hum. Mov. Sci.*, vol. 20(4–5), pp. 401–26, 2001.

U. H. Buzzi, N. Stergiou, M. J. Kurz, P. A. Hageman and J. Heidel, "Nonlinear dynamics indicates aging affects variability during gait", *Clin. Biomech.*, vol. 18(5), pp. 435–43, 2003.

M. G. Carpenter, J. H. Allum and F. Horegger, "Directional sensitivity of stretch reflexes and balance corrections for normal subjects in the roll and pitch planes", *Exp. Brain Res.*, vol. 129(1), pp. 93–113, 1999.

R. B. Chan, "A method for estimating center of mass from force plate data during quiet standing", *Proc. IEEE Bio. Med. Eng. Soci.(BMES)/Eng. Med. Bilo. Soci.(EMBS)*, pp. 516, 1999.

A. Chipperfield, P. Flemming, H. Pohlheim and C. Fonsesca, "Genetic Algorithm Toolbox for use with Matlab: User's Guide", Department of Automatic Control and Systems Engineering, University of Sheffield, v. 1.2.

C. Y. Cho and G. Kamen, "Detecting balance deficits in frequent fallers using clinical and quantitative evaluation tools", *J. Am. Geriatr. Soc.*, vol. 46(4), pp. 426–30, 1998.

J. J. Collins and C. J. De Luca, "Open-loop and closed loop control of posture: a random-walk analysis of center-of-pressure trajectories", *Exp. Brain Res.*, vol. 95(2), pp. 308–18, 1993.

H. S. M. Coxeter, "Conics." §8.4 in *Introduction to Geometry, 2nd ed.* New York: Wiley, pp. 115–9, 1969.

L. S. Chou, K. R. Kaufman, M. E. Hahn, R. H. Brey, "Medio-lateral motion of the center of mass during obstacle crossing distinguishes elderly individuals with imbalance", *Gait Posture*, vol. 18(3), pp. 125–33, 2003.

H. C. Diener, F. B. Horak and L. M. Nashner, "Influence of stimulus parameters on human postural responses", *J. Neurophysiol.*, vol. 59(6), pp. 1888–905, 1988.

V. Dietz, M. Trippel, I. K. Ibrahim and W. Berger, "Human stance on a sinusoidally translating platform: balance control by feedforward and feedback mechanisms", *Exp. Brain Res.*, vol. 93(2), pp. 352–62, 1993.

J. B. Dingwell, J. P. Cusumano, D. Sternad and P. R. Cavanagh, "Slower speeds in patients with diabetic neuropathy lead to improved local dynamic stability of continuous overground walking", *J. Biomech.*, vol. 33(10), pp. 1269–77, 2000.

T. L. A. Doyle, E. L. Dugan, B. Humphries and R. U. Newton, "Discriminating between elderly and young using a fractal dimension analysis of center of pressure", *Int. J. Med. Sci.*, vol. 1(1), pp. 11–20, 2004.

A. Gabell and U. S. Nayak, "The effect of age on variability in gait", *J. Gerontol.*, vol. 39, pp. 662–6, 1984.

P. Gatev, S. Thomas, T. Kepple and M. Hallet, "Feedforward ankle strategy of balance during quiet stance in adult", *J. Physiol.*, vol. 514(3), pp. 915–28, 1999.

J. Gill, J. H. J. Allum, M. G. Carpenter, M. H. Ziolkowska, A. L. Adkin, F. Honegger, and K. Pierchala, "Trunk sway measures of postural stability during clinical balance tests: effects of age" *J. Gerontol. A Biol. Sci. Med. Sci.*, vol. 56(7), pp. M438–47, 2001.

P. C. Grabiner, S. T. Biswas and M. D. Grabiner, "Age-related changes in spatial and temporal gait variables", *Arch. Phys. Med. Rehabil.*, vol. 82(1), pp. 31–5, 2001.

S. L. Greenspan, E. R. Myers, D. P. Kiel, R. A. Parker, W. C. Hayes and N. M. Resnick, "Fall direction, bone mineral density, and function: risk factors for hip fracture in frail nursing home elderly", *Am. J. Med.*, vol. 104, pp. 539–45, 1998.

J. Han, Z. Moussavi, T. Szturm and V. Goodman, "Application of nonlinear dynamics to human postural control system", *Proc. IEEE Eng. Med. Biol. Soc. (EMBS)*, pp. 6885–8, 2005.

J. M. Hausdorff, D. E. Forman, Z. Ladin, A. L. Goldberger, D. R. Rigney and J. Y. Wei, "Increased walking variability in elderly persons with congestive heart failure", *J. Am. Geriatr. Soc.*, vol. 42(10), pp. 1056–61, 1994.

J. M. Hausdorff, H. K. Edelberg, S. L. Mitchell, A. L. Goldberger and J. Y. Wei., "Increased gait unsteadiness in community-dwelling elderly fallers", *Arch. Phys. Med. Rehabil.*, vol. 78(3), pp. 278–383, 1997.

J. M. Hausdorff, Y. Ashkenazy, C. K. Peng, P. C. Ivanov, H. E. Stanley and A. L. Goldberger, "When human walking becomes random walking: fractal analysis and modeling of gait rhythm fluctuations", *Physica A*, vol. 302(1–4), pp. 138–47, 2001.

S. M. Henry, J. Fung and F. B. Horak, "Control of stance during lateral and anterior/posterior surface translations", *IEEE Trans. Rehabil. Eng.*, vol 6(1), 32–42, 1998.

T. Higuchi, "Approach to an irregular time series on the basis of the fractal theory", *Physica D*, vol. 31, pp. 277–83, 1988.

F. E. Huxham, P. A. Goldie and A. E. Patla, "Theoretical considerations in balance assessment", *Aust. J. Physiother.*, vol. 47(2), pp. 89–100, 2001.

T. Ito, T. Azuma and N. Yamashita, "Anticipatory control in the initiation of a single step under biomechanical constraints in humans", *Neurosci. Lett.*, vol. 352(3), pp. 207–10, 2003.

J. J. Jeka and J. R. Lackner, "The role of haptic cues from rough and slippery surfaces in human postural control", *Exp. Brain Res.*, vol. 103(2), pp. 267–76, 1995.

M. J. Katz, "Fractals and the analysis of waveforms", *Comput. Biol. Med.*, vol. 18(3), pp. 145–56, 1988.

S. Kirkpatrick, C. D. Gelatt Jr. and M. P. Vecchi, "Optimization by Simulated Annealing", *Science*, vol. 220(4598), pp. 671–80, 1983.

Y. G. Ko, J. H. Challis and K. M. Newell, "Postural coordination patterns as a function of dynamics of the support surface", *Hum. Mov. Sci.*, vol. 20(6), pp. 737–64, 2001.

A. D. Kuo, "The relative roles of feedforward and feedback in the control of rhythmic movements", *Motor Control*, vol. 6(2), pp. 129–45, 2002.

D. Lafond, M. Duarte and F. Prince, "Comparison of three methods to estimate the center of mass during balance assessment", *J. Biomech.*, vol. 37(9), pp. 1421–6, 2004.

Y. Lajoie, N. Teasdale, C. Bard and M. Fleury, "Attentional demands for static and dynamic equilibrium", *Exp. Brain Res.*, vol. 97(1), pp. 139–44, 1993.

M. J. MacLellan and A. E. Patla, "Adaptations of walking pattern on a compliant surface to regulate dynamic stability", *Exp. Brain Res.*, vol. 173, pp. 521–30, 2006.

B. E. Maki, "Gait changes in older adults: predictors of falls or indicators of fear?", *J. Am. Geriatr. Soc.*, vol. 45, pp. 313–20, 1997.

B. E. Maki, W. E. McIlroy, S. D. Perry, "Influence of lateral destabilization on compensatory stepping responses", *J. Biomech.*, vol. 29(3), pp. 343–53, 1996.

H. B. Menz, S. R. Lord and R. C. Fitzpatrik, "Acceleration pattern of the head and pelvis when walking on level and irregular surfaces", *Gait Posture*, vol. 18, pp. 35–46, 2003a.

H. B. Menz, S. R. Lord and R. C. Fitzpatrik, "Acceleration pattern of the head and pelvis when walking are associated with risk of falling in community dwelling older people", *J. Gerontol. A Biol. Sci. Med. Sci.*, vol. 58(5), pp. 446–52, 2003b.

H. B. Menz, S. R. Lord and R. C. Fitzpatrik, "Age-related differences in the walking stability", *Age and Aging*, vol. 32, pp. 137–42, 2003c.

N. Metropolis, A.W. Rosenbluth, M. N. Rosenbluth, A. H. Teller and E. Teller, "Equation of State Calculations by Fast Computing Machines", *J. Chem. Phys.*, vol. 21(6), pp. 1087–92, 1953.

Z. Michalewicz, *Genetic Algorithms + Data Structures = Evolution Programs*. Springer-Verlag., 3rd edition, part 1, 1996.

J. Mickelborough, M. L. van der Linden, R. C. Tallis and A. R. Ennos, "Muscle activity during gait initiation in normal elderly people", *Gait Posture*, vol. 19(1), pp. 50–7, 2004.

M. L. Mille, M. W. Rogers, K. Martinez, L. D. Hedman, M. E. Johnson, S. R. Lord and R. C. Fitzpatrick, "Thresholds for inducing protective stepping responses to external perturbation of human standing", *J. Neurophysiol.*, vol. 90(2), pp. 666–74, 2003.

R. Moe-Nilssen and J. L. Helbostad, "Interstride trunk acceleration variability but not step width variability can differentiate between fit and frail older adults", *Gait Posture*, vol. 21(2), pp. 164–70, 2005.

L. M. Nashner, "A model describing vestibular detection of body sway motion", *Acta Otolaryngol.*, vol. 72(6), pp. 429–36, 1971.

K. M. Newell and D. M. Corcos, "Variability and motor control", In *Issues in variability and motor control* edited by K. M. Newell and D. M. Corcos, Champaign: Human kinetics, pp. 1–12, 1993.

Y. C. Pai, J. Wening, E. F. Runtz, K. Iqbal and M. J. Pavol, "Role of feedforward control of movement stability in reducing slip-related balance loss and falls among older adults", *J. Neurophysiol.*, vol. 90(2), pp. 755–62, 2003.

M. J. Pavol and Y. C. Pai, "Feedforward adaptations are used to compensate for a potential loss of balance", *Exp. Brain Res.*, vol. 145(4), pp. 528–38, 2002.

R. J. Peterka, "Sensorimotor integration in human postural control", *J. Neurophysiol.*, vol. 88, pp. 1097–118, 2002.

R. J. Peterka and F. O. Black, "Age-related changes in human postural control: sensory organization tests", *J. Vestib. Res.*, vol. 1(1), pp. 73–85, 1990–91.

L. R. Rabiner, "A tutorial on hidden Markov models and selected applications in speech recognition", *Proc. IEEE*, vol. 77(2), pp. 257–286, 1989.

M. S. Redfern, P. L. Moore and C. M. Yarsky, "The influence of flooring on standing balance among older persons", *Hum. Factors*, vol. 39(3), pp. 445–55, 1997.

M. W. Rogers, L. D. Hedman, M. E. Johnson, T. D. Cain and T. A. Hanke, "Lateral stability during forward–induced stepping for dynamic balance recovery in young and older adults", *J. Gerontol. A Biol. Sci. Med. Sci.*, vol. 56A(9), M589–94, 2001.

M. E. Rogers, J. E. Fernandez and R. M. Bohlken, "Methods to access and improve the physical parameters associated with fall risk in older adults", *Prev. Med.*, vol. 36(3), 255–64, 2003.

C. F. Runge, C. L. Shupert, F. B. Horak and F. E. Zajac, "Ankle and hip postural strategies defined by joint torques", *Gait. Posture*, vol. 10(2), pp. 161–70, 1999.

C. F. Runge, C. L. Shupert, F. B. Horak and F. E. Zajac, "Role of vestibular information in initiation of rapid postural responses", *Exp. Brain Res.*, vol. 122(4), pp. 403–12, 1998.

M. Schiepatti, A. Giordano and A. Nardone, "Variability in dynamic postural task attests ample flexibility in balance control mechanisms", *Exp. Brain Res.*, vol. 144(2), pp. 200–10, 2002.

V. Scott, M. Pearce and C. Pengelly, "Report on senior's falls in Canada", *Public Health Agency of Canada*, 2005.

N. Sekiya, H. Nagasaki, H. Ito and T. Furuna, "Optimal walking in terms of variability in step length", *J. Orthop. Sports. Phys. Ther.*, vol. 26(5), pp. 266–72, 1997.

G. Shan, G. Wu and L. Haugh, "A method to determine the interdependent relationships between biomechanical variables in articial neural network models: the case of lower extremity muscle activity and body sway", *Neurocomputing*, vol. 61, pp. 241–58, 2004.

A. Shumway-Cook and F. B. Horak, "Assessing the influence of sensory interaction on balance", *Phys. Ther.*, vol. 66, pp. 1548–50, 1986.

Statistics Toolbox for use with MATLAB: User's Guide (version 5.0), The MathWorks, Natick, MA, USA, 2004.

H. Stolze, H. J. Friedrich, K. Steinauer and P. Vieregge, "Stride parameters in healthy young and old women - measurement variability on a simple walkway", *Exp. Aging. Res.*, vol. 26(2), pp. 159–68, 2000.

T. Szturm and B. Fallang, "Effects of varying acceleration of platform translation and toes-up rotations on the pattern and magnitude of balance reactions in humans", *J. Vestibul. Res.*, vol. 8(5), pp. 381–97, 1998.

N. Teasdale, G. E. Stelmach, and A. Breunig, "Postural sway characteristics of the elderly under normal and altered visual and support surface conditions", *J. Gerontol.*, vol. 46(6), pp. B238–44, 1991.

N. Yamada, "Chaotic swaying of the upright posture", *Hum. Movement Sci.*, vol. 14, pp. 711–26, 1995.

D. A. Winter, "Human balance and posture control during standing and walking", *Gait Posture*, vol. 3, pp. 193–214, 1995.

G. Wu and Z. Ladin, "The study of kinematic transients in locomotion using the integrated kinematic sensor", *IEEE Trans. Rehabil. Eng.*, vol. 4(3), pp. 193–200, 1996.